ESAIM: COCV 20 (2014) 1025–1058
DOI: 10.1051/cocv/2014006

ESAIM: Control, Optimisation and Calculus of Variations
www.esaim-cocv.org

RELATING PHASE FIELD AND SHARP INTERFACE APPROACHES TO STRUCTURAL TOPOLOGY OPTIMIZATION

Luise Blank[1], Harald Garcke[1], M. Hassan Farshbaf-Shaker[2] and Vanessa Styles[3]

Abstract. A phase field approach for structural topology optimization which allows for topology changes and multiple materials is analyzed. First order optimality conditions are rigorously derived and it is shown *via* formally matched asymptotic expansions that these conditions converge to classical first order conditions obtained in the context of shape calculus. We also discuss how to deal with triple junctions where *e.g.* two materials and the void meet. Finally, we present several numerical results for mean compliance problems and a cost involving the least square error to a target displacement.

Mathematics Subject Classification. 49Q10, 74P10, 49Q20, 74P05, 65M60.

Received March 8, 2013. Revised January 10, 2014.
Published online August 5, 2014.

1. Introduction

In structural topology optimization one tries to distribute a limited amount of material in a design domain such that an objective functional is minimized. Known quantities in these problems are *e.g.* the applied loads, possible support conditions, the volume of the structure and possible restrictions as for example prescribed solid regions or given holes. *A priori* the precise shape and the connectivity (the "topology") of the structure is not known. Often also the problem arises that several materials have to be distributed in the given design domain.

Different methods have been used to deal with shape and topology optimization problems. The classical method uses boundary variations in order to compute shape derivatives which can be used to decrease the objective functional by deforming the boundary of the shape in a descent direction, see *e.g.* [41, 53, 54] and the references therein. The boundary variation technique has the drawback that it needs high computational costs and does not allow for a change of topology.

Keywords and phrases. Structural topology optimization, linear elasticity, phase-field method, first order conditions, matched asymptotic expansions, shape calculus, numerical simulations.

[1] Fakultät für Mathematik, Universität Regensburg, 93040 Regensburg, Germany. luise.blank@mathematik.uni-regensburg.de; harald.garcke@mathematik.uni-regensburg.de

[2] Weierstrass Institute for Applied Analysis and Stochastics, Mohrenstrasse 39, 10117 Berlin, Germany. Hassan.Farshbaf-Shaker@wias-berlin.de

[3] Department of Mathematics, University of Sussex, Brighton, BN1 9QH, UK. v.styles@sussex.ac.uk

Article published by EDP Sciences

© EDP Sciences, SMAI 2014

https://doi.org/10.1051/cocv/2014006 Published online by Cambridge University Press

Sometimes one can deal with the change of topology by using homogenization methods, see [2] and variants of it such as the SIMP method, see [7] and the reference therein. These approaches are restricted to special classes of objective functionals.

Another approach which was very popular in the last ten years is the level set method which was originally introduced in [45]. The level set method allows for a change of topology and was successfully used for topology optimization by many authors, see *e.g.* [17, 44]. Nevertheless for some problems the level set method has difficulties to create new holes. To overcome this problem the sensitivity with respect to the opening of a small hole is expressed by so called topological derivatives, see [54]. Then, the topological derivative can be incorporated into the level set method, see *e.g.* [18], in order to create new holes.

The principal objective in shape and topology optimization is to find regions which should be filled by material in order to optimize an objective functional. In a parametric approach this is done by a parametrization of the boundary of the material region and in the optimization process the boundary is varied. In a level set method the boundary is described by a level set function and in the optimization process the level set function changes in order to optimize the objective. As the boundary of the region filled by material is unknown the shape optimization problem is a free boundary problem. Another way to handle free boundary problems and interface problems is the phase field method which has been used for many different free boundary type problems, see *e.g.* [20, 23].

In structural optimization problems the phase field approach has been used by different authors [9, 11, 12, 16, 24, 50, 55, 58–61]. The phase field method is capable of handling topology changes and also the nucleation of new holes is possible, see *e.g.* [9]. The method is applied for domain dependent loads [11], multi-material structural topology optimization [60], minimization of the least square error to a target displacement [55], topology optimization with local stress constraints [18], mean compliance optimization [9, 55], compliant mechanism design problems [55], eigenfrequency maximization problems [55] and problems involving nonlinear elasticity [50].

Although many computational results on phase field approaches to topology optimization exist there has been relatively little work on analytical aspects. One result to be mentioned is the Γ-convergence result, see *e.g.* [11], which relates the phase field energy in topology optimization to classical objective functionals. There is an existence result for the phase field model for compliance shape optimization in nonlinear elasticity in [50]. Most other authors derived first order conditions in a formal way and presented numerical examples obtained by a gradient flow method leading to either an Allen−Cahn [9] or a Cahn−Hilliard type phase field equation [24, 55, 60]. We also like to mention that in [16] a primal-dual interior point method is used to solve the phase field topological optimization problem.

Although in principle the phase field approach can also be applied for other problems in topology optimization we focus on applications formulated in the context of linear elasticity. In the simplest situation given a working or design domain Ω with a boundary $\partial\Omega$ which is decomposed into a Dirichlet part Γ_D, a non-homogeneous Neumann part Γ_g and a homogeneous Neumann part Γ_0 and body and surface forces $\boldsymbol{f}$ and $\boldsymbol{g}$ one tries to find a domain $\Omega^M \subset \Omega$ (M stands for material) and the displacement $\boldsymbol{u}$ such that the mean compliance

$$\int_{\Omega^M} \boldsymbol{f} \cdot \boldsymbol{u} + \int_{\Gamma_g \cap \partial\Omega^M} \boldsymbol{g} \cdot \boldsymbol{u}$$

or the error compared to a target displacement $\boldsymbol{u}_\Omega$, *i.e.*

$$\left(\int_{\Omega^M} c|\boldsymbol{u} - \boldsymbol{u}_\Omega|^2 \right)^\nu, \ \nu \in (0, 1]$$

is minimized, where c is a given weighting function and $|\cdot|$ is the Euclidean norm. In the paper of Allaire *et al.* [3] besides other choices the case $\nu = \frac{1}{2}$ was considered and the case $\nu = 1$ leads to a least square minimization problem. This is the reason why we consider a range of possible choices for ν. Later we add the perimeter functional to the functional and then the minima will depend on ν. Here the displacement $\boldsymbol{u}$ is the solution of

https://doi.org/10.1051/cocv/2014006 Published online by Cambridge University Press

the linearized elasticity system

$$-\nabla \cdot \left(\mathbb{C}^M \mathcal{E}(\boldsymbol{u})\right) = \boldsymbol{f} \text{ in } \Omega^M$$

subject to appropriate boundary conditions. As discussed in [3] the above minimization problem is not well-posed on the set of all possible shapes and typically a perimeter regularization is used, *i.e.* one adds

$$P(\Omega^M) = \int_{(\partial\Omega^M)\cap\Omega} \mathrm{d}s$$

to the above functionals, where ds stands for the surface measure.

In a phase field model the domains with material and the void are described by a phase field $\boldsymbol{\varphi}$ which attains two given values. Moreover the interface between the domains is not sharp any longer but diffuse where the thickness of the interface is proportional to a small parameter ε. The phase field rapidly changes in an interfacial region. Then the perimeter is approximated by a suitable multiple of

$$\int_\Omega \left(\tfrac{\varepsilon}{2}|\nabla\boldsymbol{\varphi}|^2 + \frac{1}{\varepsilon}\Psi(\boldsymbol{\varphi}) \right),$$

where Ψ is a potential function attaining global minima at given values of $\boldsymbol{\varphi}$ which correspond to void and material. We refer to the next section for a precise formulation of the problem.

In this paper we first give a precise formulation of the problem also in the case of multi-material structural topology optimization (Sect. 2). In this context we use ideas introduced in [30, 60]. Then we rigorously derive first order optimality conditions (Sect. 4). In Section 5 we consider the sharp interface limit of the first order conditions, *i.e.* we take the limit $\varepsilon \to 0$ and therefore the thickness of the interface converges to zero. We obtain limiting equations with the help of formally matched asymptotic expansions and relate the limit, which involve classical terms from shape calculus, transmission conditions and triple junction conditions, to the shape calculus of [3].

Finally we present several numerical computations by using a gradient descent method based on a volume conserving L^2-gradient flow of the energy. The resulting problem is a generalized non-local vector-valued Allen−Cahn variational inequality coupled to elasticity. We solve this evolution equation using a primal dual active set method as in [8].

2. Formulation of the problem

In this subsection we first introduce the phase field method and after that we will formulate the structural topology optimization problem in the phase field context.

2.1. Phase field approach

Given a bounded Lipschitz design domain $\Omega \subset \mathbb{R}^d$ we describe the material distribution with the help of a phase field vector $\boldsymbol{\varphi} := (\varphi^i)_{i=1}^N$, where each component of $\boldsymbol{\varphi}$ stands for the fraction of one material. Hence, d denotes the dimension of our working domain Ω and N stands for the number of materials. Moreover we denote by φ^N the fraction of void. We consider systems in which the total spatial amount of phases are prescribed, *e.g.* we have additionally the constraint $⨍_\Omega \boldsymbol{\varphi} = \boldsymbol{m} = (m^i)_{i=1}^N$, where $m^i \in (0,1)$ for $i \in \{1,\dots,N\}$ is a fixed given number. We use the notation $⨍_\Omega f(x)\mathrm{d}x := \frac{1}{|\Omega|}f(x)\mathrm{d}x$ with $|\Omega|$ being the Lebesgue measure of Ω. To ensure that all phases are present we require $0 < m^i < 1$ and $\sum_{i=1}^N m^i = 1$, where the last condition makes sure that $\sum_{i=1}^N \varphi^i = 1$ can be true. We define $\mathbb{R}^N_+ := \{\boldsymbol{v} \in \mathbb{R}^N \mid \boldsymbol{v} \geq \boldsymbol{0}\}$, where $\boldsymbol{v} \geq \boldsymbol{0}$ means $v^i \geq 0$ for all $i \in \{1,\dots,N\}$, the affine hyperplane

$$\Sigma^N := \left\{ \boldsymbol{v} \in \mathbb{R}^N \mid \sum_{i=1}^N v^i = 1 \right\},$$

https://doi.org/10.1051/cocv/2014006 Published online by Cambridge University Press

and its tangent plane

$$T\Sigma^N := \left\{ \boldsymbol{v} \in \mathbb{R}^N \mid \sum_{i=1}^{N} v^i = 0 \right\}.$$

With these definitions we obtain as the phase space for the order parameter $\boldsymbol{\varphi}$ the Gibbs simplex $\boldsymbol{G} = \mathbb{R}^N_+ \cap \Sigma^N$. We furthermore define $\boldsymbol{\mathcal{G}} := \{\boldsymbol{v} \in H^1(\Omega, \mathbb{R}^N) \mid \boldsymbol{v}(x) \in \boldsymbol{G} \text{ a.e. in } \Omega\}$ and $\boldsymbol{\mathcal{G}^m} := \{\boldsymbol{v} \in \boldsymbol{\mathcal{G}} \mid \fint_\Omega \boldsymbol{v} = \boldsymbol{m}\}$. As discussed in the introduction we use the well-known Ginzburg–Landau energy

$$E^\varepsilon(\boldsymbol{\varphi}) := \int_\Omega \left(\frac{\varepsilon}{2} |\nabla \boldsymbol{\varphi}|^2 + \frac{1}{\varepsilon} \Psi(\boldsymbol{\varphi}) \right), \qquad \varepsilon > 0, \tag{2.1}$$

which is an approximation of the weighted perimeter functional. The choice of E^ε as an approximation of surface energy goes back to van der Waals [57] and was also used by Cahn and Hilliard [19] in order to derive the Cahn−Hilliard equation. In minimization problems the term $\frac{1}{\varepsilon}\Psi(\boldsymbol{\varphi})$ requires that $\boldsymbol{\varphi}$ attains values close to the global minima of Ψ. If several global minima of Ψ exist the function $\boldsymbol{\varphi}$ possibly jumps between the minima. It turns out that without the gradient term there is no restriction on the size of the jump set. However, the term $\frac{\varepsilon}{2}|\nabla \boldsymbol{\varphi}|^2$ penalizes interfacial regions and therefore the size of the jump set. Hence the overall functional can be interpreted as an approximation of interfacial area. In fact Modica [40] for the scalar case and later Baldo [4] for the vector-valued case were able to show that the functional E^ε converges to the perimeter functional. The convergence theory of the Ginzburg–Landau energy E^ε for $\varepsilon \to 0$ relies on the notion of Γ-convergence, see [4, 40].

In (2.1) the function $\Psi : \mathbb{R}^N \to \mathbb{R} \cup \{\infty\}$ is a bulk potential with a N-well structure on Σ^N, *i.e.* with exactly N global minima $\boldsymbol{e}_i$ ($i \in \{1, \dots, N\}$) and height $\Psi(\boldsymbol{e}_i) = 0$, where $\boldsymbol{e}_i$ is the ith unit vector in $\mathbb{R}^N$. In this paper we use obstacle functionals of the form $\Psi(\boldsymbol{\varphi}) = \Psi_0(\boldsymbol{\varphi}) + I_{\boldsymbol{G}}(\boldsymbol{\varphi})$, where $\Psi_0 \in C^{1,1}(\mathbb{R}^N, \mathbb{R})$ and $I_{\boldsymbol{G}}$ is the indicator function of $\boldsymbol{G}$, *i.e.*

$$I_{\boldsymbol{G}}(\boldsymbol{\varphi}) := \begin{cases} 0 & \text{for } \boldsymbol{\varphi} \in \boldsymbol{G}, \\ \infty & \text{otherwise.} \end{cases}$$

Prototype examples for Ψ_0 are given by

$$\Psi_0(\boldsymbol{\varphi}) := \frac{1}{2}(1 - \boldsymbol{\varphi} \cdot \boldsymbol{\varphi}) \quad \text{and} \quad \Psi_0(\boldsymbol{\varphi}) := \frac{1}{2} \boldsymbol{\varphi} \cdot \mathcal{W} \boldsymbol{\varphi}, \tag{2.2}$$

where $\mathcal{W}$ is a symmetric $N \times N$ matrix [10, 25] with zeros on the diagonal which in addition is negative definite on $T\Sigma^N$. On Σ^N we have $(1 - \boldsymbol{\varphi} \cdot \boldsymbol{\varphi}) = \boldsymbol{\varphi} \cdot (\mathbf{1} \otimes \mathbf{1} - Id)\boldsymbol{\varphi}$ with $\mathbf{1} = (1, \dots, 1)^T$ and hence on Σ^N the first choice is a special case of the second.

We remark that on $\boldsymbol{\mathcal{G}}$ we have

$$E^\varepsilon(\boldsymbol{\varphi}) = \int_\Omega \left(\frac{\varepsilon}{2} |\nabla \boldsymbol{\varphi}|^2 + \frac{1}{\varepsilon} \Psi_0(\boldsymbol{\varphi}) \right) =: \hat{E}^\varepsilon(\boldsymbol{\varphi}). \tag{2.3}$$

This observation is important for the analysis in Section 4.

We denote by $\boldsymbol{u} : \Omega \to \mathbb{R}^d$ the displacement vector and by

$$\mathcal{E} := \mathcal{E}(\boldsymbol{u}) := (\nabla \boldsymbol{u})^{\text{sym}}$$

the strain tensor, where $\mathcal{A}^{\text{sym}} := \frac{1}{2}(\mathcal{A} + \mathcal{A}^T)$ is the symmetric part of a second order tensor $\mathcal{A}$. Furthermore, we denote by $\mathbb{C}$ the elasticity tensor, by $\boldsymbol{f} : \Omega \to \mathbb{R}^d$ a vector-valued volume force and by $\boldsymbol{g} : \Gamma_g \to \mathbb{R}^d$ a boundary traction acting on the structure. In this paper we always assume $\boldsymbol{f} \in L^2(\Omega, \mathbb{R}^d)$ and $\boldsymbol{g} \in L^2(\Gamma_g, \mathbb{R}^d)$. The boundary of our domain is divided into a Dirichlet part Γ_D with positive $(d-1)$-dimensional Hausdorff

https://doi.org/10.1051/cocv/2014006 Published online by Cambridge University Press

measure, *i.e.* $\mathcal{H}^{d-1}(\Gamma_D) > 0$ and a Neumann part, which consists of a non-homogeneous Neumann part Γ_g and a homogeneous Neumann part Γ_0. Moreover, in our setting the elasticity equation which is used in structural topology optimization is given by

$$\begin{cases} -\nabla \cdot [\mathbb{C}(\boldsymbol{\varphi})\mathcal{E}(\boldsymbol{u})] = \left(1-\varphi^N\right)\boldsymbol{f} & \text{in } \Omega, \\ \boldsymbol{u} = \boldsymbol{0} & \text{on } \Gamma_D, \\ [\mathbb{C}(\boldsymbol{\varphi})\mathcal{E}(\boldsymbol{u})]\,\boldsymbol{n} = \boldsymbol{g} & \text{on } \Gamma_g, \\ [\mathbb{C}(\boldsymbol{\varphi})\mathcal{E}(\boldsymbol{u})]\,\boldsymbol{n} = \boldsymbol{0} & \text{on } \Gamma_0, \end{cases} \tag{2.4}$$

where $\boldsymbol{n}$ is the outer unit normal to $\partial\Omega = \Gamma_D \cup \Gamma_g \cup \Gamma_0$. Introducing the notation

$$\langle \mathcal{A}, \mathcal{B} \rangle_{\mathbb{C}} := \int_\Omega \mathcal{A} : \mathbb{C}\mathcal{B},$$

where for any matrices $\mathcal{A}$ and $\mathcal{B}$ the product is given as $\mathcal{A} : \mathcal{B} := \sum_{i,j=1}^d \mathcal{A}_{\mathrm{ij}}\mathcal{B}_{\mathrm{ij}}$, the elastic boundary value problem (2.4) can be written in the weak formulation

$$\langle \mathcal{E}(\boldsymbol{u}), \mathcal{E}(\boldsymbol{\eta}) \rangle_{\mathbb{C}(\boldsymbol{\varphi})} = F(\boldsymbol{\eta}, \boldsymbol{\varphi}), \tag{2.5}$$

which has to hold for all $\boldsymbol{\eta} \in H^1_D(\Omega, \mathbb{R}^d) := \{\boldsymbol{\eta} \in H^1(\Omega, \mathbb{R}^d) \mid \boldsymbol{\eta} = \boldsymbol{0} \text{ on } \Gamma_D\}$ and where

$$F(\boldsymbol{\eta}, \boldsymbol{\varphi}) = \int_\Omega \left(1-\varphi^N\right)\boldsymbol{f} \cdot \boldsymbol{\eta} + \int_{\Gamma_g} \boldsymbol{g} \cdot \boldsymbol{\eta}. \tag{2.6}$$

The assumptions on the elasticity tensor are $\mathbb{C}_{\mathrm{ijkl}} \in C^{1,1}(\mathbb{R}^N, \mathbb{R})$, $i,j,k,l \in \{1,\dots,d\}$, and the symmetry property

$$\mathbb{C}_{\mathrm{ijkl}} = \mathbb{C}_{\mathrm{jikl}} = \mathbb{C}_{\mathrm{ijlk}} = \mathbb{C}_{\mathrm{klij}}$$

holds. Additionally, there exist positive constants $\theta, \Lambda, \Lambda'$, such that for all symmetric matrices $\mathcal{A}, \mathcal{B} \in \mathbb{R}^{d\times d}\setminus\{\boldsymbol{0}\}$ and for all $\boldsymbol{\varphi}, \boldsymbol{h} \in \mathbb{R}^N$ it holds

$$\theta|\mathcal{A}|^2 \le \mathbb{C}(\boldsymbol{\varphi})\mathcal{A} : \mathcal{A} \le \Lambda|\mathcal{A}|^2, \tag{2.7}$$

$$|\mathbb{C}'(\boldsymbol{\varphi})\boldsymbol{h}\mathcal{A} : \mathcal{B}| \le \Lambda'|\boldsymbol{h}||\mathcal{A}||\mathcal{B}|, \tag{2.8}$$

where $\mathbb{C}'(\boldsymbol{\varphi})\boldsymbol{h} := \left(\sum_{m=1}^N \partial_m \mathbb{C}_{\mathrm{ijkl}}(\boldsymbol{\varphi})h_m\right)_{i,j,k,l=1}^d$.

More information on the theory of elasticity can be found in the books [21, 37]. Discussions on appropriate interpolations $\mathbb{C}(\boldsymbol{\varphi})$ of the elasticity tensors in the pure material can be found in [7, 28, 30, 34]. In the following we discuss a concrete choice of the interpolation function, which fulfills the above assumptions.

2.2. Choice of the elasticity tensor

We now discuss how we can define a $\boldsymbol{\varphi}$-dependent elasticity tensor starting with constant elasticity tensors $\mathbb{C}^i$, $i \in \{1,\dots,N-1\}$ which are defined in the pure materials, *i.e.* when $\boldsymbol{\varphi} = \boldsymbol{e}_i$. We first extend the elasticity tensor to the Gibbs simplex, then define it on the hyperplane Σ^N and eventually on the whole of $\mathbb{R}^N$. First of all we model the void as a very soft material. A possible choice which is appropriate for the sharp interface limit discussed later and for the numerics is $\mathbb{C}^N = \mathbb{C}^N(\varepsilon) = \varepsilon^2\tilde{\mathbb{C}}^N$, where $\tilde{\mathbb{C}}^N$ is a fixed elasticity tensor. For the sharp interface analysis it is only necessary that $\mathbb{C}^N(\varepsilon) = \mathcal{O}(\varepsilon)$. However, a quadratic rate in ε accelerates the convergence in the void as $\varepsilon \to 0$ and is hence chosen in the numerical computations. Moreover, we assume that there exist positive constants $\tilde{\vartheta}_i, \vartheta_i$ such that for all $\mathcal{A} \in \mathbb{R}^{d\times d} \setminus \{\boldsymbol{0}\}$ it holds

$$\vartheta_i|\mathcal{A}|^2 \le \mathbb{C}^i\mathcal{A} : \mathcal{A} \le \tilde{\vartheta}_i|\mathcal{A}|^2 \quad \forall i \in \{1,\dots,N\}. \tag{2.9}$$

https://doi.org/10.1051/cocv/2014006 Published online by Cambridge University Press

In order to model the elastic properties also in the interfacial region the elasticity tensor is assumed to be a tensor valued function $\mathbb{C}(\boldsymbol{\varphi}) := (\mathbb{C}_{ijkl}(\boldsymbol{\varphi}))_{i,j,k,l=1}^{d}$ and we set for $\boldsymbol{\varphi}$ in the Gibbs simplex

$$\mathbb{C}(\boldsymbol{\varphi}) = \overline{\mathbb{C}}(\boldsymbol{\varphi}) + \mathbb{C}^N \varphi^N, \quad \forall \boldsymbol{\varphi} \in \boldsymbol{G}, \tag{2.10}$$

where $\overline{\mathbb{C}}(\boldsymbol{\varphi}) := \sum_{i=1}^{N-1} \mathbb{C}^i \varphi^i$.

We now extend the elasticity tensor $\mathbb{C}$ to the hyperplane Σ^N. For $\delta > 0$ we define on $\mathbb{R}$ a monotone $C^{1,1}$-function

$$w(s) := \begin{cases} -\delta & \text{for} \quad s < -\delta, \\ w_l(s) & \text{for} \quad -\delta \le s < 0, \\ s & \text{for} \quad 0 \le s \le 1, \\ w_r(s) & \text{for} \quad 1 < s \le 1+\delta, \\ 1+\delta & \text{for} \quad s > 1+\delta, \end{cases} \tag{2.11}$$

where w_j, $j \in \{l, r\}$ are monotone $C^{1,1}$-functions such that $w \in C^{1,1}$. By means of (2.11) we construct an extension of the elasticity tensor $\mathbb{C}(\boldsymbol{\varphi})$ for $\boldsymbol{\varphi}$ in the affine hyperplane Σ^N

$$\hat{\mathbb{C}}(\boldsymbol{\varphi}) = \sum_{i=1}^{N} \mathbb{C}^i w(\varphi^i), \quad \forall \boldsymbol{\varphi} \in \Sigma^N. \tag{2.12}$$

Indeed for $\boldsymbol{\varphi} \in \boldsymbol{G}$ we have $w(\varphi^i) = \varphi^i$, $\forall i \in \{1, \dots, N\}$ and $\hat{\mathbb{C}}(\boldsymbol{\varphi}) = \mathbb{C}(\boldsymbol{\varphi})$, *i.e.* in the Gibbs simplex we have a linear interpolation of the values in the corners of the simplex. Such linear interpolations are frequently used in the modeling of multi-phase elasticity, see [28,34]. For $\boldsymbol{\varphi} \in \Sigma^N$ we obtain

$$\begin{aligned} \hat{\mathbb{C}}(\boldsymbol{\varphi})\mathcal{A} : \mathcal{A} &= \sum_{i=1}^{N} w(\varphi^i) \mathbb{C}^i \mathcal{A} : \mathcal{A} \\ &= \sum_{i \in I_{<0}} w(\varphi^i) \mathbb{C}^i \mathcal{A} : \mathcal{A} + \sum_{i \in I_{\ge 0}} w(\varphi^i) \mathbb{C}^i \mathcal{A} : \mathcal{A}, \end{aligned} \tag{2.13}$$

where the index sets are defined as

$$I_{<0} := \{i \in \{1, \dots, N\} \mid \varphi^i < 0\}; \quad I_{\ge 0} := \{1, \dots, N\} \setminus I_{<0}.$$

Hence, we obtain, using $\sum_{i \in I_{\ge 0}} \varphi^i \ge 1$,

$$\hat{\mathbb{C}}(\boldsymbol{\varphi})\mathcal{A} : \mathcal{A} \ge \left[\min_{i \in I_{\ge 0}} \vartheta_i - \delta \max_{i \in I_{<0}} \tilde{\vartheta}_i |I_{<0}|) \right] |\mathcal{A}|^2.$$

Choosing δ small enough there exists a $\delta' > 0$ such that for all $|I_{<0}|$

$$\left[\min_{i \in I_{\ge 0}} \vartheta_i - \delta \max_{i \in I_{<0}} \tilde{\vartheta}_i |I_{<0}|) \right] \ge \delta'$$

and we can set $\theta := \delta'$ in (2.7).

We now define the projection from $\mathbb{R}^N$ into Σ^N by

$$P_\Sigma(\boldsymbol{\varphi}) = \operatorname*{arg\,min}_{\boldsymbol{v} \in \Sigma^N} \frac{1}{2} \|\boldsymbol{\varphi} - \boldsymbol{v}\|_{l^2}^2, \quad \forall \boldsymbol{\varphi} \in \mathbb{R}$$

and define an extension $\check{\mathbb{C}}$ of $\hat{\mathbb{C}}$ as follows

$$\check{\mathbb{C}}(\boldsymbol{\varphi}) = \sum_{i=1}^{N} \mathbb{C}^i w\left(P_\Sigma(\boldsymbol{\varphi})^i\right), \quad \forall \boldsymbol{\varphi} \in \mathbb{R}^N. \tag{2.14}$$

Then $\check{\mathbb{C}}(\boldsymbol{\varphi})$ fulfills (2.7) and (2.8).

https://doi.org/10.1051/cocv/2014006 Published online by Cambridge University Press

2.3. Structural optimization problem

In the following we are going to formulate an optimization problem involving the mean compliance functional (2.6) and the functional for the compliant mechanism, which is given by

$$J_0(\boldsymbol{u},\boldsymbol{\varphi}) := \left(\int_\Omega c\,\left(1-\varphi^N\right)|\boldsymbol{u}-\boldsymbol{u}_\Omega|^2\right)^\nu, \qquad \nu\in(0,1], \tag{2.15}$$

with a target displacement $\boldsymbol{u}_\Omega$ and a given non-negative weighting factor $c\in L^\infty(\Omega)$ with $|\operatorname{supp} c|>0$, where $|\operatorname{supp} c|$ is the Lebesgue measure of $\operatorname{supp} c$.

Given $(\boldsymbol{f},\boldsymbol{g},\boldsymbol{u}_\Omega,c)\in L^2(\Omega,\mathbb{R}^d)\times L^2(\Gamma_g,\mathbb{R}^d)\times L^2(\Omega,\mathbb{R}^d)\times L^\infty(\Omega)$ and measurable sets $S_i\subseteq\Omega$, $i\in\{0,1\}$, with $S_0\cap S_1=\emptyset$, the overall optimization problem is

$$(\mathcal{P}^\varepsilon)\qquad \begin{cases} \min & J^\varepsilon(\boldsymbol{u},\boldsymbol{\varphi}) := \alpha F(\boldsymbol{u},\boldsymbol{\varphi})+\beta J_0(\boldsymbol{u},\boldsymbol{\varphi})+\gamma E^\varepsilon(\boldsymbol{\varphi}),\\ \text{over} & (\boldsymbol{u},\boldsymbol{\varphi})\in H^1_D(\Omega,\mathbb{R}^d)\times H^1(\Omega,\mathbb{R}^N),\\ \text{s.t.} & (2.5)\text{ is fulfilled and }\boldsymbol{\varphi}\in\boldsymbol{\mathcal{G}}^{\boldsymbol{m}}\cap\boldsymbol{U}_c, \end{cases}$$

where $\alpha,\beta\geq 0$, $\gamma,\varepsilon>0$, $\boldsymbol{m}\in(0,1)^N\cap\Sigma^N$ and

$$\boldsymbol{U}_c := \{\boldsymbol{\varphi}\in H^1(\Omega,\mathbb{R}^N)\mid \varphi^N=0 \text{ a.e. on } S_0 \text{ and } \varphi^N=1 \text{ a.e. on } S_1\}.$$

Remark 2.1.

(i) From the applicational point of view it is desirable to fix material or void in some regions of the design domain, so the condition $\boldsymbol{\varphi}\in\boldsymbol{U}_c$ makes sense. Moreover by choosing S_0 such that $|S_0\cap\operatorname{supp} c|\neq 0$ we can ensure that it is not possible to choose only void on the support of c, *i.e.* in (2.15) $|\operatorname{supp}(1-\varphi^N)\cap\operatorname{supp} c|>0$.

(ii) Taking (2.1) and (2.3) into account we can replace $E^\varepsilon(\boldsymbol{\varphi})$ by $\hat{E}^\varepsilon(\boldsymbol{\varphi})$ in $(\mathcal{P}^\varepsilon)$.

3. Analysis of the state equation

In this section we discuss the well-posedness of the state equation (2.4) and show the differentiability of the control-to-state operator. In this section the functions $(\boldsymbol{f},\boldsymbol{g})\in L^2(\Omega,\mathbb{R}^d)\times L^2(\Gamma_g,\mathbb{R}^d)$ are given. Because $(\boldsymbol{\mathcal{G}}^{\boldsymbol{m}}\cap\boldsymbol{U}_c)\subset L^\infty(\Omega,\mathbb{R}^N)$ we assume throughout this section that $\boldsymbol{\varphi}\in L^\infty(\Omega,\mathbb{R}^N)$.

Theorem 3.1. *For any given $\boldsymbol{\varphi}\in L^\infty(\Omega,\mathbb{R}^N)$ there exists a unique $\boldsymbol{u}\in H^1_D(\Omega,\mathbb{R}^d)$ which fulfills (2.5). Furthermore, there exists a positive constant C which depends on the data of the problem such that*

$$\|\boldsymbol{u}\|_{H^1_D(\Omega,\mathbb{R}^d)}\leq C(\|\boldsymbol{\varphi}\|_{L^\infty(\Omega,\mathbb{R}^N)}+1). \tag{3.1}$$

Proof. Indeed $\langle\mathcal{E}(\cdot),\mathcal{E}(\cdot)\rangle_{\mathbb{C}(\boldsymbol{\varphi})}: H^1_D(\Omega,\mathbb{R}^d)\times H^1_D(\Omega,\mathbb{R}^d)\to\mathbb{R}$ is a bilinear form and we have by (2.7) and Korn's inequality, see [63] Corollary 62.13 and [38,43],

$$\langle\mathcal{E}(\boldsymbol{u}),\mathcal{E}(\boldsymbol{u})\rangle_{\mathbb{C}(\boldsymbol{\varphi})}\geq\frac{\theta}{c_K}\|\boldsymbol{u}\|^2_{H^1_D(\Omega,\mathbb{R}^d)} \qquad \forall\boldsymbol{u}\in H^1_D(\Omega,\mathbb{R}^d), \tag{3.2}$$

where $c_K>0$ stems from Korn's inequality. Hence, $\langle\mathcal{E}(\cdot),\mathcal{E}(\cdot)\rangle_{\mathbb{C}(\boldsymbol{\varphi})}$ is $H^1_D(\Omega,\mathbb{R}^d)$-elliptic. Moreover, using (2.7) it is easy to check that $\langle\cdot,\cdot\rangle_{\mathbb{C}(\boldsymbol{\varphi})}$ is continuous. Applying Hölder's inequality and the trace theorem we have

$$\begin{aligned}|F(\boldsymbol{\eta},\boldsymbol{\varphi})| &\leq \int_\Omega|(1-\varphi^N)\boldsymbol{f}\cdot\boldsymbol{\eta}|+\int_{\Gamma_g}|\boldsymbol{g}\cdot\boldsymbol{\eta}|\\ &\leq C\left(\|1-\varphi^N\|_{L^\infty(\Omega)}\|\boldsymbol{f}\|_{L^2(\Omega,\mathbb{R}^d)}+\|\boldsymbol{g}\|_{L^2(\Gamma_g,\mathbb{R}^d)}\right)\|\boldsymbol{\eta}\|_{H^1_D(\Omega,\mathbb{R}^d)},\end{aligned} \tag{3.3}$$

where $C>0$. Hence, for $\boldsymbol{\varphi}\in L^\infty(\Omega,\mathbb{R}^N)$ it holds that $F(\cdot,\boldsymbol{\varphi})\in(H^1_D(\Omega,\mathbb{R}^d))^*$. Applying the Lax–Milgram theorem we obtain a unique solution $\boldsymbol{u}\in H^1_D(\Omega,\mathbb{R}^d)$ to (2.5) and (3.1) follows from (3.3) and (3.2). □

https://doi.org/10.1051/cocv/2014006 Published online by Cambridge University Press

Based on Theorem 3.1 we define the solution or the control-to-state operator

$$S : L^\infty(\Omega, \mathbb{R}^N) \to H^1_D(\Omega, \mathbb{R}^d), \quad S(\boldsymbol{\varphi}) := \boldsymbol{u}, \tag{3.4}$$

which assigns to a given control $\boldsymbol{\varphi} \in L^\infty(\Omega, \mathbb{R}^N)$ the unique state variable $\boldsymbol{u} \in H^1_D(\Omega, \mathbb{R}^d)$.

In order to derive first-order necessary optimality conditions for the optimization problem $(\mathcal{P}^\varepsilon)$, it is essential to show the differentiability of the control-to-state operator S. In order to show this we prove the following stability result.

Theorem 3.2. *Let $M > 0$ and suppose that $\boldsymbol{\varphi}_i \in L^\infty(\Omega, \mathbb{R}^N)$ with $\|\boldsymbol{\varphi}_i\|_{L^\infty(\Omega,\mathbb{R}^N)} \le M$, $i = 1, 2$, are given. For $\boldsymbol{u}_i = S(\boldsymbol{\varphi}_i)$, $i = 1, 2$, there exists a positive constant C which depends on the given data of the problem and on M such that*

$$\|\boldsymbol{u}_1 - \boldsymbol{u}_2\|_{H^1_D(\Omega,\mathbb{R}^d)} \le C \|\boldsymbol{\varphi}_1 - \boldsymbol{\varphi}_2\|_{L^\infty(\Omega,\mathbb{R}^N)}. \tag{3.5}$$

Proof. Because of $\boldsymbol{u}_i = S(\boldsymbol{\varphi}_i) \in H^1_D(\Omega, \mathbb{R}^d)$ it holds

$$\langle \mathcal{E}(\boldsymbol{u}_i), \mathcal{E}(\boldsymbol{\eta}) \rangle_{\mathbb{C}(\boldsymbol{\varphi}_i)} = F(\boldsymbol{\eta}, \boldsymbol{\varphi}_i) \qquad \forall \boldsymbol{\eta} \in H^1_D(\Omega, \mathbb{R}^d), \tag{3.6}$$

where $i = 1, 2$. The difference gives

$$\int_\Omega [\mathbb{C}(\boldsymbol{\varphi}_1)\mathcal{E}(\boldsymbol{u}_1) - \mathbb{C}(\boldsymbol{\varphi}_2)\mathcal{E}(\boldsymbol{u}_2)] : \mathcal{E}(\boldsymbol{\eta}) = \int_\Omega \left(\varphi_2^N - \varphi_1^N\right) \boldsymbol{f} \cdot \boldsymbol{\eta} \qquad \forall \boldsymbol{\eta} \in H^1_D\left(\Omega, \mathbb{R}^d\right). \tag{3.7}$$

Testing (3.7) with $\boldsymbol{\eta} := \boldsymbol{u}_1 - \boldsymbol{u}_2 \in H^1_D(\Omega, \mathbb{R}^d)$, using

$$[\mathbb{C}(\boldsymbol{\varphi}_1)\mathcal{E}(\boldsymbol{u}_1) - \mathbb{C}(\boldsymbol{\varphi}_2)\mathcal{E}(\boldsymbol{u}_2)] = [\mathbb{C}(\boldsymbol{\varphi}_1) - \mathbb{C}(\boldsymbol{\varphi}_2)]\,\mathcal{E}(\boldsymbol{u}_2) + \mathbb{C}(\boldsymbol{\varphi}_1)\mathcal{E}(\boldsymbol{u}_1 - \boldsymbol{u}_2)$$

and (2.7) we get for (3.7)

$$\begin{aligned} \theta \|\mathcal{E}(\boldsymbol{u}_1 - \boldsymbol{u}_2)\|^2_{L^2(\Omega,\mathbb{R}^{d\times d})} &\le \langle \mathcal{E}(\boldsymbol{u}_1 - \boldsymbol{u}_2), \mathcal{E}(\boldsymbol{u}_1 - \boldsymbol{u}_2) \rangle_{\mathbb{C}(\boldsymbol{\varphi}_1)} \\ &\le \left| \int_\Omega [\mathbb{C}(\boldsymbol{\varphi}_1) - \mathbb{C}(\boldsymbol{\varphi}_2)] \mathcal{E}(\boldsymbol{u}_2) : \mathcal{E}(\boldsymbol{u}_1 - \boldsymbol{u}_2) \right| \\ &\quad + \left| \int_\Omega (\varphi_2^N - \varphi_1^N) \boldsymbol{f} \cdot (\boldsymbol{u}_1 - \boldsymbol{u}_2) \right|. \end{aligned}$$

Because of Hölder's inequality and the global Lipschitz-continuity of $\mathbb{C}$ we obtain

$$\begin{aligned} \theta \|\mathcal{E}(\boldsymbol{u}_1 - \boldsymbol{u}_2)\|^2_{L^2(\Omega,\mathbb{R}^{d\times d})} &\le L_{\mathbb{C}} \|\boldsymbol{\varphi}_1 - \boldsymbol{\varphi}_2\|_{L^\infty(\Omega,\mathbb{R}^N)} \|\mathcal{E}(\boldsymbol{u}_2)\|_{L^2(\Omega,\mathbb{R}^{d\times d})} \|\mathcal{E}(\boldsymbol{u}_1 - \boldsymbol{u}_2)\|_{L^2(\Omega,\mathbb{R}^{d\times d})} \\ &\quad + \|\boldsymbol{\varphi}_1 - \boldsymbol{\varphi}_2\|_{L^\infty(\Omega,\mathbb{R}^N)} \|\boldsymbol{f}\|_{L^2(\Omega,\mathbb{R}^d)} \|\boldsymbol{u}_1 - \boldsymbol{u}_2\|_{L^2(\Omega,\mathbb{R}^d)}, \end{aligned} \tag{3.8}$$

where $L_{\mathbb{C}}$ denotes the global Lipschitz-constant. Using (3.1), Korn's inequality, the inequality (3.8) finally shows (3.5). □

We are now in a position to prove the differentiability of the control-to-state operator.

Theorem 3.3. *The control-to-state operator S, defined in (3.4), is Fréchet differentiable. Its directional derivative at $\boldsymbol{\varphi} \in L^\infty(\Omega, \mathbb{R}^N)$ in the direction $\boldsymbol{h} \in L^\infty(\Omega, \mathbb{R}^N)$ is given by*

$$S'(\boldsymbol{\varphi})\boldsymbol{h} = \boldsymbol{u}^*, \tag{3.9}$$

where $\boldsymbol{u}^*$ denotes the unique solution of the problem

$$\langle \mathcal{E}(\boldsymbol{u}^*), \mathcal{E}(\boldsymbol{\eta}) \rangle_{\mathbb{C}(\boldsymbol{\varphi})} = -\langle \mathcal{E}(\boldsymbol{u}), \mathcal{E}(\boldsymbol{\eta}) \rangle_{\mathbb{C}'(\boldsymbol{\varphi})\boldsymbol{h}} - \int_\Omega h^N \boldsymbol{f} \cdot \boldsymbol{\eta}, \ \forall \boldsymbol{\eta} \in H^1_D(\Omega, \mathbb{R}^d) \tag{3.10}$$

where $\boldsymbol{u} = S(\boldsymbol{\varphi})$.

https://doi.org/10.1051/cocv/2014006 Published online by Cambridge University Press

Remark 3.4. Formally equation (3.10) can be derived by differentiating the implicit state equation

$$\langle \mathcal{E}(S(\boldsymbol{\varphi})), \mathcal{E}(\boldsymbol{\eta})\rangle_{\mathbb{C}(\boldsymbol{\varphi})} = F(\boldsymbol{\eta}, \boldsymbol{\varphi})$$

with respect to $\boldsymbol{\varphi} \in L^\infty(\Omega, \mathbb{R}^N)$. Moreover, there exists a constant $C > 0$ which depends on the given data of the problem such that the estimate

$$\|\boldsymbol{u}^*\|_{H^1_D(\Omega,\mathbb{R}^d)} \leq C\|\boldsymbol{h}\|_{L^\infty(\Omega,\mathbb{R}^N)} \tag{3.11}$$

holds, which shows that $S'(\boldsymbol{\varphi})$ is a bounded operator.

Proof of Theorem 3.3. For given $\boldsymbol{h} \in L^\infty(\Omega, \mathbb{R}^N)$ we define

$$\hat{F}(\boldsymbol{\eta}, \boldsymbol{h}) := -\langle \mathcal{E}(\boldsymbol{u}), \mathcal{E}(\boldsymbol{\eta})\rangle_{\mathbb{C}'(\boldsymbol{\varphi})\boldsymbol{h}} - \int_\Omega h^N \boldsymbol{f} \cdot \boldsymbol{\eta}, \quad \forall \boldsymbol{\eta} \in H^1_D(\Omega, \mathbb{R}^d).$$

Using (2.8) we can estimate

$$\begin{aligned} |\hat{F}(\boldsymbol{\eta}, \boldsymbol{h})| &\leq |\langle \mathcal{E}(\boldsymbol{u}), \mathcal{E}(\boldsymbol{\eta})\rangle_{\mathbb{C}'(\boldsymbol{\varphi})\boldsymbol{h}}| + \int_\Omega |h^N \boldsymbol{f} \cdot \boldsymbol{\eta}| \\ &\leq \max\{\Lambda', 1\}\|\boldsymbol{h}\|_{L^\infty(\Omega,\mathbb{R}^N)}(\|\boldsymbol{f}\|_{L^2(\Omega,\mathbb{R}^d)} + \|\boldsymbol{u}\|_{H^1_D(\Omega,\mathbb{R}^d)})\|\boldsymbol{\eta}\|_{H^1_D(\Omega,\mathbb{R}^d)}. \end{aligned}$$

By (3.1) we can estimate $\|\boldsymbol{u}\|_{H^1_D(\Omega,\mathbb{R}^d)}$ and we obtain that $\hat{F}(\cdot, \boldsymbol{h}) \in (H^1_D(\Omega, \mathbb{R}^d))^*$. Hence, the existence of a unique solution $\boldsymbol{u}^* \in H^1_D(\Omega, \mathbb{R}^d)$ to (3.10) is given by the Lax−Milgram theorem.

Now define $\boldsymbol{u}^{\boldsymbol{h}} := S(\boldsymbol{\varphi} + \boldsymbol{h})$ and $\boldsymbol{r} := \boldsymbol{u}^{\boldsymbol{h}} - \boldsymbol{u} - \boldsymbol{u}^*$, where $\boldsymbol{u}^*$ fulfills (3.10). We have to show that

$$\|\boldsymbol{r}\|_{H^1_D(\Omega,\mathbb{R}^d)} = o(\|\boldsymbol{h}\|_{L^\infty(\Omega,\mathbb{R}^N)}) \qquad \text{as } \|\boldsymbol{h}\|_{L^\infty(\Omega,\mathbb{R}^N)} \to 0. \tag{3.12}$$

Applying the definition of $\boldsymbol{u}$, $\boldsymbol{u}^{\boldsymbol{h}}$ and $\boldsymbol{u}^*$ we obtain

$$\langle \mathcal{E}(\boldsymbol{u}^{\boldsymbol{h}}), \mathcal{E}(\boldsymbol{\eta})\rangle_{\mathbb{C}(\boldsymbol{\varphi}+\boldsymbol{h})} - \langle \mathcal{E}(\boldsymbol{u}), \mathcal{E}(\boldsymbol{\eta})\rangle_{\mathbb{C}(\boldsymbol{\varphi})} - \langle \mathcal{E}(\boldsymbol{u}^*), \mathcal{E}(\boldsymbol{\eta})\rangle_{\mathbb{C}(\boldsymbol{\varphi})} = \langle \mathcal{E}(\boldsymbol{u}), \mathcal{E}(\boldsymbol{\eta})\rangle_{\mathbb{C}'(\boldsymbol{\varphi})\boldsymbol{h}}, \ \forall \boldsymbol{\eta} \in H^1_D(\Omega, \mathbb{R}^d).$$

Using

$$[\mathbb{C}(\boldsymbol{\varphi} + \boldsymbol{h})\mathcal{E}(\boldsymbol{u}^{\boldsymbol{h}}) - \mathbb{C}(\boldsymbol{\varphi})\mathcal{E}(\boldsymbol{u})] = [\mathbb{C}(\boldsymbol{\varphi} + \boldsymbol{h}) - \mathbb{C}(\boldsymbol{\varphi})]\mathcal{E}(\boldsymbol{u}^{\boldsymbol{h}}) + \mathbb{C}(\boldsymbol{\varphi})\mathcal{E}(\boldsymbol{u}^{\boldsymbol{h}} - \boldsymbol{u}), \tag{3.13}$$

we obtain after standard calculations

$$\begin{aligned} \langle \mathcal{E}(\boldsymbol{r}), \mathcal{E}(\boldsymbol{\eta})\rangle_{\mathbb{C}(\boldsymbol{\varphi})} = &- \langle \mathcal{E}(\boldsymbol{u}^{\boldsymbol{h}}), \mathcal{E}(\boldsymbol{\eta})\rangle_{\mathbb{C}(\boldsymbol{\varphi}+\boldsymbol{h})-\mathbb{C}(\boldsymbol{\varphi})-\mathbb{C}'(\boldsymbol{\varphi})\boldsymbol{h}} \\ &- \langle \mathcal{E}(\boldsymbol{u}^{\boldsymbol{h}} - \boldsymbol{u}), \mathcal{E}(\boldsymbol{\eta})\rangle_{\mathbb{C}'(\boldsymbol{\varphi})\boldsymbol{h}}, \quad \forall \boldsymbol{\eta} \in H^1_D(\Omega, \mathbb{R}^d). \end{aligned} \tag{3.14}$$

Now we choose $\boldsymbol{\eta} := \boldsymbol{r}$ in (3.14). Using (2.7) for the left side of (3.14) we have

$$|\langle \mathcal{E}(\boldsymbol{r}), \mathcal{E}(\boldsymbol{r})\rangle_{\mathbb{C}(\boldsymbol{\varphi})}| \geq \theta\|\mathcal{E}(\boldsymbol{r})\|^2_{L^2(\Omega,\mathbb{R}^{d\times d})}. \tag{3.15}$$

Due to the differentiability properties of $\mathbb{C}$, see Section 2, we obtain

$$\begin{aligned} |\mathbb{C}(\boldsymbol{\varphi} + \boldsymbol{h}) - \mathbb{C}(\boldsymbol{\varphi}) - \mathbb{C}'(\boldsymbol{\varphi})\boldsymbol{h}| &\leq |\boldsymbol{h}| \int_0^1 |\mathbb{C}'(\boldsymbol{\varphi} + t\boldsymbol{h}) - \mathbb{C}'(\boldsymbol{\varphi})|\mathrm{d}t \\ &\leq \frac{1}{2} L_{\mathbb{C}'} |\boldsymbol{h}|^2, \end{aligned} \tag{3.16}$$

https://doi.org/10.1051/cocv/2014006 Published online by Cambridge University Press

where we used for the last estimate the global Lipschitz-continuity of $\mathbb{C}'$ with the Lipschitz constant $L_{\mathbb{C}'}$. We obtain using Hölder's inequality for the first summand of the right hand side of (3.14)

$$\begin{aligned}|\langle \mathcal{E}(\boldsymbol{u}^{\boldsymbol{h}}), \mathcal{E}(\boldsymbol{r})\rangle_{\mathbb{C}(\boldsymbol{\varphi}+\boldsymbol{h})-\mathbb{C}(\boldsymbol{\varphi})-\mathbb{C}'(\boldsymbol{\varphi})\boldsymbol{h}}| \leq & L_{\mathbb{C}'}\|\boldsymbol{h}\|^2_{L^\infty(\Omega,\mathbb{R}^N)}\cdot \\ & \cdot \|\mathcal{E}(\boldsymbol{u}^{\boldsymbol{h}})\|_{L^2(\Omega,\mathbb{R}^{d\times d})}\|\mathcal{E}(\boldsymbol{r})\|_{L^2(\Omega,\mathbb{R}^{d\times d})}. \end{aligned} \tag{3.17}$$

Owing to (3.1), we can estimate $\|\mathcal{E}(\boldsymbol{u}^{\boldsymbol{h}})\|_{L^2(\Omega,\mathbb{R}^{d\times d})}$ in (3.17). For the second summand on the right hand side of (3.14) with $\boldsymbol{\eta} := \boldsymbol{r}$ we obtain using (2.8)

$$\begin{aligned}|\langle \mathcal{E}(\boldsymbol{u}^{\boldsymbol{h}} - \boldsymbol{u}), \mathcal{E}(\boldsymbol{r})\rangle_{\mathbb{C}'(\boldsymbol{\varphi})\boldsymbol{h}}| \leq & \Lambda'\|\boldsymbol{h}\|_{L^\infty(\Omega,\mathbb{R}^N)}\cdot \\ & \|\mathcal{E}(\boldsymbol{u}^{\boldsymbol{h}} - \boldsymbol{u})\|_{L^2(\Omega,\mathbb{R}^{d\times d})}\|\mathcal{E}(\boldsymbol{r})\|_{L^2(\Omega,\mathbb{R}^{d\times d})}.\end{aligned}$$

Moreover, (3.5) yields $\|\mathcal{E}(\boldsymbol{u}^{\boldsymbol{h}} - \boldsymbol{u})\|_{L^2(\Omega,\mathbb{R}^{d\times d})} \leq C\|\boldsymbol{h}\|_{L^\infty(\Omega,\mathbb{R}^N)}$ and we get that there exists a positive constant C such that

$$|\langle \mathcal{E}(\boldsymbol{u}^{\boldsymbol{h}} - \boldsymbol{u}), \mathcal{E}(\boldsymbol{r})\rangle_{\mathbb{C}'(\boldsymbol{\varphi})\boldsymbol{h}}| \leq C\|\boldsymbol{h}\|^2_{L^\infty(\Omega,\mathbb{R}^N)}\|\mathcal{E}(\boldsymbol{r})\|_{L^2(\Omega,\mathbb{R}^{d\times d})}. \tag{3.18}$$

Using (3.15), (3.17) and (3.18) this establishes (3.12). We now want to prove (3.11). Testing (3.10) with $\boldsymbol{\eta} := \boldsymbol{u}^*$ and arguing like in the proof of Theorem 3.2 we end up with (3.11) and hence we proved Theorem 3.3. □

4. Optimal control problem

The goal of this section is to show that the minimization problem $(\mathcal{P}^\varepsilon)$ has a solution and to derive first-order necessary optimality conditions. In this section $(\boldsymbol{f}, \boldsymbol{g}, \boldsymbol{u}_\Omega, c) \in L^2(\Omega,\mathbb{R}^d) \times L^2(\Gamma_g,\mathbb{R}^d) \times L^2(\Omega,\mathbb{R}^d) \times L^\infty(\Omega)$ and measurable sets $S_i \subseteq \Omega$, $i \in \{0,1\}$, with $S_0 \cap S_1 = \emptyset$, are given.

Theorem 4.1. *The problem $(\mathcal{P}^\varepsilon)$ has a minimizer.*

Proof. We denote the feasible set by

$$\mathcal{F}_{\text{ad}} := \left\{(\boldsymbol{u},\boldsymbol{\varphi}) \in H^1_D(\Omega,\mathbb{R}^d) \times (\boldsymbol{\mathcal{G}}^{\boldsymbol{m}} \cap \boldsymbol{U}_c) \mid (\boldsymbol{u},\boldsymbol{\varphi}) \text{ fulfills } (2.5)\right\}.$$

Using (2.5) with $\boldsymbol{\eta} = \boldsymbol{u}$ it is clear that J^ε is bounded from below on $\mathcal{F}_{\text{ad}}$. Since $\mathcal{F}_{\text{ad}}$ is nonempty, the infimum

$$\inf_{(\boldsymbol{u},\boldsymbol{\varphi})\in\mathcal{F}_{\text{ad}}} J^\varepsilon(\boldsymbol{u},\boldsymbol{\varphi})$$

exists and hence we find a minimizing sequence $\{(\boldsymbol{u}_k,\boldsymbol{\varphi}_k)\} \subset \mathcal{F}_{\text{ad}}$ with

$$\lim_{k\to\infty} J^\varepsilon(\boldsymbol{u}_k,\boldsymbol{\varphi}_k) = \inf_{(\boldsymbol{u},\boldsymbol{\varphi})\in\mathcal{F}_{\text{ad}}} J^\varepsilon(\boldsymbol{u},\boldsymbol{\varphi}).$$

Moreover, we obtain, using (3.1), that there exists a positive constant C such that

$$J^\varepsilon(\boldsymbol{u}_k,\boldsymbol{\varphi}_k) \geq \gamma\frac{\varepsilon}{2}\|\nabla\boldsymbol{\varphi}_k\|^2_{L^2(\Omega)} - C.$$

Hence, by virtue of $⨍_\Omega \boldsymbol{\varphi}_k = \boldsymbol{m}$ for all $k \in \mathbb{N}$ and the Poincaré inequality the sequence $\{\boldsymbol{\varphi}_k\} \subset (\boldsymbol{\mathcal{G}}^{\boldsymbol{m}} \cap \boldsymbol{U}_c)$ is bounded in $H^1(\Omega,\mathbb{R}^N) \cap L^\infty(\Omega,\mathbb{R}^N)$. Theorem 3.1 implies that also the sequence of the corresponding states $\{\boldsymbol{u}_k\} \subset H^1_D(\Omega,\mathbb{R}^d)$ is bounded. Hence there exist some $(\overline{\boldsymbol{u}},\overline{\boldsymbol{\varphi}}) \in H^1_D(\Omega,\mathbb{R}^d) \times H^1(\Omega,\mathbb{R}^N)$ and subsequences (also denoted the same) such that as $k \to \infty$

$$\begin{aligned}\boldsymbol{u}_k &\longrightarrow \overline{\boldsymbol{u}} \quad \text{weakly in } H^1_D(\Omega,\mathbb{R}^d), \\ \boldsymbol{\varphi}_k &\longrightarrow \overline{\boldsymbol{\varphi}} \quad \text{weakly in } H^1(\Omega,\mathbb{R}^N).\end{aligned} \tag{4.1}$$

https://doi.org/10.1051/cocv/2014006 Published online by Cambridge University Press

Moreover the set $\boldsymbol{\mathcal{G}^m} \cap \boldsymbol{U}_c$ is convex and closed, hence weakly closed and we get $(\overline{\boldsymbol{u}}, \overline{\boldsymbol{\varphi}}) \in H^1_D(\Omega, \mathbb{R}^d) \times (\boldsymbol{\mathcal{G}^m} \cap \boldsymbol{U}_c)$. Finally we have to show that J^ε is sequentially weakly lower semi-continuous. From the above convergence result we obtain for $k \to \infty$

$$\begin{aligned} \boldsymbol{u}_k &\longrightarrow \overline{\boldsymbol{u}} \quad \text{strongly in } L^2(\Omega, \mathbb{R}^d), \\ \boldsymbol{\varphi}_k &\longrightarrow \overline{\boldsymbol{\varphi}} \quad \text{strongly in } L^2(\Omega, \mathbb{R}^N) \end{aligned} \tag{4.2}$$

and after possibly choosing another subsequence which is again denoted by $\{k\}$ we obtain

$$\boldsymbol{\varphi}_k \longrightarrow \overline{\boldsymbol{\varphi}} \text{ a.e. in } \Omega. \tag{4.3}$$

Using (4.1), (4.2) and since the norm is weakly lower semi-continuous we immediately obtain

$$J^\varepsilon(\overline{\boldsymbol{u}}, \overline{\boldsymbol{\varphi}}) \leq \liminf_{k \to \infty} J^\varepsilon(\boldsymbol{u}_k, \boldsymbol{\varphi}_k)\,.$$

In addition (4.1), (4.2), (4.3) and the fact that $(\boldsymbol{u}_k, \boldsymbol{\varphi}_k)$ fulfills (2.5) imply that also $(\overline{\boldsymbol{u}}, \overline{\boldsymbol{\varphi}})$ fulfill (2.5). For the last conclusion we have to pass to the limit in $\int_\Omega \mathbb{C}(\boldsymbol{\varphi}_k)\mathcal{E}(\boldsymbol{u}_k) : \mathcal{E}(\boldsymbol{\eta})$ as $k \to \infty$. Convergence follows due to the uniformly boundedness of $\{\boldsymbol{\varphi}_k\}$, the properties of the elasticity tensor and since (4.3) provides together with the dominated convergence theorem of Lebesgue strong convergence of $\mathbb{C}(\boldsymbol{\varphi}_k)\mathcal{E}(\boldsymbol{\eta})$ to $\mathbb{C}(\overline{\boldsymbol{\varphi}})\mathcal{E}(\boldsymbol{\eta})$ in $L^2(\Omega, \mathbb{R}^{d\times d})$. Using moreover (4.1) we obtain

$$\int_\Omega \mathbb{C}(\boldsymbol{\varphi}_k)\mathcal{E}(\boldsymbol{u}_k) : \mathcal{E}(\boldsymbol{\eta}) \longrightarrow \int_\Omega \mathbb{C}(\overline{\boldsymbol{\varphi}})\mathcal{E}(\overline{\boldsymbol{u}}) : \mathcal{E}(\boldsymbol{\eta}) \quad \forall \boldsymbol{\eta} \in H^1_D\left(\Omega, \mathbb{R}^d\right).$$

The above discussion shows

$$-\infty < \inf_{(\boldsymbol{u},\boldsymbol{\varphi}) \in \mathcal{F}_{\text{ad}}} J^\varepsilon(\boldsymbol{u}, \boldsymbol{\varphi}) \leq J^\varepsilon(\overline{\boldsymbol{u}}, \overline{\boldsymbol{\varphi}}) \leq \liminf_{k \to \infty} J^\varepsilon(\boldsymbol{u}_k, \boldsymbol{\varphi}_k) = \inf_{(\boldsymbol{u},\boldsymbol{\varphi}) \in \mathcal{F}_{\text{ad}}} J^\varepsilon(\boldsymbol{u}, \boldsymbol{\varphi}).$$

Therefore $(\overline{\boldsymbol{u}}, \overline{\boldsymbol{\varphi}}) \in H^1_D(\Omega, \mathbb{R}^d) \times (\boldsymbol{\mathcal{G}^m} \cap \boldsymbol{U}_c)$ is a minimizer of $(\mathcal{P}^\varepsilon)$. □

4.1. Fréchet-differentiability of the reduced functional

For the rest of the paper we assume that, in case $\beta \neq 0$ and $\nu \in (0, 1]$ we only consider $(\boldsymbol{u}, \boldsymbol{\varphi})$ such that $\tilde{J}_0(\boldsymbol{u}, \boldsymbol{\varphi}) := \int_\Omega c(1 - \varphi^N)|\boldsymbol{u} - \boldsymbol{u}_\Omega|^2 \neq 0$. This will guarantee that $J_0 = (\tilde{J}_0)^\nu$ is differentiable. In case $\nu = 1$ we set $J_0(\boldsymbol{u}, \boldsymbol{\varphi})^{\frac{\nu-1}{\nu}} = (\tilde{J}_0)^{\nu-1} = 1$ even if $J_0 = 0$.

In the following, $\boldsymbol{\varphi} \in H^1(\Omega, \mathbb{R}^N) \cap L^\infty(\Omega, \mathbb{R}^N)$ and $\boldsymbol{u} = S(\boldsymbol{\varphi}) \in H^1_D(\Omega, \mathbb{R}^d)$ is the associated state. With the control-to-state operator $S : H^1(\Omega, \mathbb{R}^N) \cap L^\infty(\Omega, \mathbb{R}^N) \subset L^\infty(\Omega, \mathbb{R}^N) \to H^1_D(\Omega, \mathbb{R}^d)$ the cost functional thus attains the form

$$\begin{aligned} J^\varepsilon(\boldsymbol{u}, \boldsymbol{\varphi}) &= J^\varepsilon(S(\boldsymbol{\varphi}), \boldsymbol{\varphi}) \\ &= \alpha F(S(\boldsymbol{\varphi}), \boldsymbol{\varphi}) + \beta J_0(S(\boldsymbol{\varphi}), \boldsymbol{\varphi}) + \gamma \hat{E}^\varepsilon(\boldsymbol{\varphi}) =: j(\boldsymbol{\varphi}), \end{aligned} \tag{4.4}$$

where F, J_0 and $\hat{E}^\varepsilon$ are defined as in (2.6), (2.15) and (2.3). The Fréchet-differentiability of the reduced cost-functional j in $H^1(\Omega, \mathbb{R}^N) \cap L^\infty(\Omega, \mathbb{R}^N)$ is shown in the next lemma.

Lemma 4.2. *The reduced cost-functional $j : H^1(\Omega, \mathbb{R}^N) \cap L^\infty(\Omega, \mathbb{R}^N) \to \mathbb{R}$ is Fréchet-differentiable.*

Proof. We first show that $J^\varepsilon : H^1_D(\Omega, \mathbb{R}^d) \times (H^1(\Omega, \mathbb{R}^N) \cap L^\infty(\Omega, \mathbb{R}^N)) \to \mathbb{R}$ is Fréchet differentiable. It is an easy task to formally calculate the partial derivatives of J^ε at $(\boldsymbol{u}, \boldsymbol{\varphi})$ in the direction $(\boldsymbol{v}, \boldsymbol{h})$. We obtain

$$\begin{aligned} J^\varepsilon_{\prime \boldsymbol{u}}(\boldsymbol{u}, \boldsymbol{\varphi})\boldsymbol{v} &= \alpha F_{\prime \boldsymbol{u}}(\boldsymbol{u}, \boldsymbol{\varphi})\boldsymbol{v} + \beta (J_0)_{\prime \boldsymbol{u}}(\boldsymbol{u}, \boldsymbol{\varphi})\boldsymbol{v}, \\ J^\varepsilon_{\prime \boldsymbol{\varphi}}(\boldsymbol{u}, \boldsymbol{\varphi})\boldsymbol{h} &= \alpha F_{\prime \boldsymbol{\varphi}}(\boldsymbol{\varphi})\boldsymbol{h} + \beta (J_0)_{\prime \boldsymbol{\varphi}}(\boldsymbol{u}, \boldsymbol{\varphi})\boldsymbol{h} + \gamma \hat{E}^\varepsilon_{\prime \boldsymbol{\varphi}}(\boldsymbol{\varphi})\boldsymbol{h}, \end{aligned} \tag{4.5}$$

https://doi.org/10.1051/cocv/2014006 Published online by Cambridge University Press

with

$$F_{\prime \boldsymbol{u}}(\boldsymbol{u},\boldsymbol{\varphi})\boldsymbol{v} = \int_\Omega \left(1-\varphi^N\right)\boldsymbol{f}\cdot\boldsymbol{v} + \int_{\Gamma_g} \boldsymbol{g}\cdot\boldsymbol{v}, \tag{4.6a}$$

$$(J_0)_{\prime \boldsymbol{u}}(\boldsymbol{u},\boldsymbol{\varphi})\boldsymbol{v} = 2\nu J_0(\boldsymbol{u},\boldsymbol{\varphi})^{\frac{\nu-1}{\nu}} \int_\Omega c\,\left(1-\varphi^N\right)(\boldsymbol{u}-\boldsymbol{u}_\Omega)\cdot\boldsymbol{v}, \tag{4.6b}$$

$$F_{\prime \boldsymbol{\varphi}}(\boldsymbol{u},\boldsymbol{\varphi})\boldsymbol{h} = -\int_\Omega h^N \boldsymbol{f}\cdot\boldsymbol{u}, \tag{4.6c}$$

$$(J_0)_{\prime \boldsymbol{\varphi}}(\boldsymbol{u},\boldsymbol{\varphi})\boldsymbol{h} = -\nu J_0(\boldsymbol{u},\boldsymbol{\varphi})^{\frac{\nu-1}{\nu}} \int_\Omega c\,h^N\,|\boldsymbol{u}-\boldsymbol{u}_\Omega|^2, \tag{4.6d}$$

$$\hat{E}^\varepsilon_{\prime \boldsymbol{\varphi}}(\boldsymbol{\varphi})\boldsymbol{h} = \varepsilon\int_\Omega \nabla\boldsymbol{\varphi} : \nabla\boldsymbol{h} + \frac{1}{\varepsilon}\int_\Omega \Psi_0'(\boldsymbol{\varphi})\cdot\boldsymbol{h}. \tag{4.6e}$$

We remark that $\boldsymbol{v}$ and $\boldsymbol{h}$ appear linearly in the integral expressions in (4.6a-e). Also, the continuity of the expressions in (4.6a-e) with respect to the directions $\boldsymbol{v}$ and $\boldsymbol{h}$ follow directly. We furthermore will show the continuity of the expressions in (4.6a-e) with respect to $(\boldsymbol{u},\boldsymbol{\varphi})$. Then the Fréchet-differentiability of J^ε follows from Proposition 4.14 of Zeidler [62].

We will only show continuity of the most difficult term in (4.6a-e) namely the term $(J_0)_{\prime \boldsymbol{u}}(\boldsymbol{u},\boldsymbol{\varphi})\boldsymbol{v}$. To this end, let $\{(\boldsymbol{u}_k,\boldsymbol{\varphi}_k)\} \subset H^1_D(\Omega,\mathbb{R}^d)\times(H^1(\Omega,\mathbb{R}^N)\cap L^\infty(\Omega,\mathbb{R}^N))$ be a given sequence such that as $k\to\infty$

$$(\boldsymbol{u}_k,\boldsymbol{\varphi}_k) \longrightarrow (\boldsymbol{u},\boldsymbol{\varphi}) \text{ in } H^1_D(\Omega,\mathbb{R}^d)\times\left(H^1(\Omega,\mathbb{R}^N)\cap L^\infty\left(\Omega,\mathbb{R}^N\right)\right) \tag{4.7}$$

and after possibly choosing a subsequence which is again denoted by an index k we can in addition assume

$$(\boldsymbol{u}_k,\boldsymbol{\varphi}_k) \longrightarrow (\boldsymbol{u},\boldsymbol{\varphi}) \quad \text{a.e. in} \quad \Omega. \tag{4.8}$$

We have to prove that for all above sequences $(\boldsymbol{u}_k,\boldsymbol{\varphi}_k)$

$$(J_0)_{\prime \boldsymbol{u}}(\boldsymbol{u}_k,\boldsymbol{\varphi}_k) \longrightarrow (J_0)_{\prime \boldsymbol{u}}(\boldsymbol{u},\boldsymbol{\varphi}) \quad \text{ as } k\to\infty \tag{4.9}$$

in the operator norm. We obtain with the help of the Cauchy–Schwarz inequality

$$\begin{aligned}\left|\left[(J_0)_{\prime \boldsymbol{u}}(\boldsymbol{u}_k,\boldsymbol{\varphi}_k) - (J_0)_{\prime \boldsymbol{u}}(\boldsymbol{u},\boldsymbol{\varphi})\right](\boldsymbol{v})\right| \le C\|&J_0(\boldsymbol{u}_k,\boldsymbol{\varphi}_k)^{\frac{\nu-1}{\nu}}(1-\varphi_k^N)(\boldsymbol{u}_k-\boldsymbol{u}_\Omega)\\ &-J_0(\boldsymbol{u},\boldsymbol{\varphi})^{\frac{\nu-1}{\nu}}(1-\varphi^N)(\boldsymbol{u}-\boldsymbol{u}_\Omega)\|_{L^2(\Omega,\mathbb{R}^d)}\,\|\boldsymbol{v}\|_{L^2(\Omega,\mathbb{R}^d)}\,.\end{aligned}$$

Using $\boldsymbol{u}_k\to\boldsymbol{u}$ in $L^2(\Omega,\mathbb{R}^d)$ and almost everywhere, the fact that $\boldsymbol{\varphi}_k\to\boldsymbol{\varphi}$ uniformly and taking the assumption at the beginning of Section 4.1 into account we obtain with the help of the generalized majorized convergence theorem of Lebesgue, see Zeidler [64],

$$\|J_0(\boldsymbol{u}_k,\boldsymbol{\varphi}_k)^{\frac{\nu-1}{\nu}}(1-\varphi_k^N)(\boldsymbol{u}_k-\boldsymbol{u}_\Omega) - J_0(\boldsymbol{u},\boldsymbol{\varphi})^{\frac{\nu-1}{\nu}}(1-\varphi^N)(\boldsymbol{u}-\boldsymbol{u}_\Omega)\|_{L^2(\Omega,\mathbb{R}^d)} \to 0 \text{ as } k\to\infty\,.$$

The facts that the control-to-state operator is Fréchet-differentiable, see Theorem 3.3, the chain rule, see [56] Theorem 2.20, give that j is Fréchet-differentiable and hence we obtain

$$j'(\boldsymbol{\varphi})\boldsymbol{h} = J^\varepsilon_{\prime \boldsymbol{u}}(\boldsymbol{u},\boldsymbol{\varphi})\boldsymbol{u}^* + J^\varepsilon_{\prime \boldsymbol{\varphi}}(\boldsymbol{u},\boldsymbol{\varphi})\boldsymbol{h}, \tag{4.10}$$

where $\boldsymbol{u}^* = S'(\boldsymbol{\varphi})\boldsymbol{h}$, see Theorem 3.3. This shows Lemma 4.2. □

https://doi.org/10.1051/cocv/2014006 Published online by Cambridge University Press

4.2. Adjoint equation

In this subsection, we discuss the following equation, which is the system formally adjoint to (2.4):

$$\begin{cases} -\nabla\cdot[\mathbb{C}(\boldsymbol{\varphi})\mathcal{E}(\boldsymbol{p})] = \alpha\left(1-\varphi^N\right)\boldsymbol{f} \\ \qquad\qquad + 2\beta\nu J_0(\boldsymbol{u},\boldsymbol{\varphi})^{\frac{\nu-1}{\nu}} c(1-\varphi^N)(\boldsymbol{u}-\boldsymbol{u}_\Omega) \ \text{ in } \Omega, \\ \qquad\qquad \boldsymbol{p} = \boldsymbol{0} \qquad\qquad \text{on } \Gamma_D, \\ [\mathbb{C}(\boldsymbol{\varphi})\mathcal{E}(\boldsymbol{p})]\,\boldsymbol{n} = \alpha\boldsymbol{g} \qquad\qquad \text{on } \Gamma_g, \\ [\mathbb{C}(\boldsymbol{\varphi})\mathcal{E}(\boldsymbol{p})]\,\boldsymbol{n} = \boldsymbol{0} \qquad\qquad \text{on } \Gamma_0. \end{cases} \tag{4.11}$$

We now show existence of a weak solution to the above problem (4.11).

Theorem 4.3. *For given* $(\boldsymbol{\varphi},\boldsymbol{u}) \in (H^1(\Omega,\mathbb{R}^N)\cap L^\infty(\Omega,\mathbb{R}^N))\times H^1_D(\Omega,\mathbb{R}^d)$ *there exists a unique* $\boldsymbol{p}\in H^1_D(\Omega,\mathbb{R}^d)$ *which fulfills* (4.11) *in the weak sense,* i.e.*,*

$$\langle\mathcal{E}(\boldsymbol{p}),\mathcal{E}(\boldsymbol{\eta})\rangle_{\mathbb{C}(\boldsymbol{\varphi})} = \tilde{F}(\boldsymbol{\eta},\boldsymbol{\varphi}) \qquad \forall\boldsymbol{\eta}\in H^1_D\left(\Omega,\mathbb{R}^d\right), \tag{4.12}$$

where

$$\tilde{F}(\boldsymbol{\eta},\boldsymbol{\varphi}) := \alpha\int_\Omega\left(1-\varphi^N\right)\boldsymbol{f}\cdot\boldsymbol{\eta} + \alpha\int_{\Gamma_g}\boldsymbol{g}\cdot\boldsymbol{\eta} + +2\beta\nu J_0(\boldsymbol{u},\boldsymbol{\varphi})^{\frac{\nu-1}{\nu}}\int_\Omega c(1-\varphi^N)(\boldsymbol{u}-\boldsymbol{u}_\Omega)\cdot\boldsymbol{\eta}.$$

Proof. One easily can check as in the proof of Theorem 3.3 that $\tilde{F}(\cdot,\boldsymbol{\varphi})\in(H^1_D(\Omega,\mathbb{R}^d))^*$ for every $\boldsymbol{\varphi}\in H^1(\Omega,\mathbb{R}^N)\cap L^\infty(\Omega,\mathbb{R}^N)$. Hence, the existence of a unique weak solution $\boldsymbol{p}\in H^1_D(\Omega,\mathbb{R}^d)$ to (4.11) is given by the Lax−Milgram theorem. □

4.3. First-order necessary optimality conditions

In the following, let $\boldsymbol{\varphi}\in\boldsymbol{\mathcal{G}}^{\boldsymbol{m}}\cap\boldsymbol{U}_c$ denote a minimizer of the problem $(\mathcal{P}^\varepsilon)$ and $\boldsymbol{u}=S(\boldsymbol{\varphi})\in H^1_D(\Omega,\mathbb{R}^d)$ is the associated state variable. Using the reduced functional j, see (4.4), the optimal control problem $(\mathcal{P}^\varepsilon)$ can be reformulated as follows

$$\min_{\boldsymbol{\varphi}\in\boldsymbol{\mathcal{G}}^{\boldsymbol{m}}\cap\boldsymbol{U}_c} j(\boldsymbol{\varphi}). \tag{4.13}$$

Lemma 4.4. *Let* $\boldsymbol{u}^*\in H^1_D(\Omega,\mathbb{R}^d)$ *be the solution to* (3.10) *and let* $\boldsymbol{p}\in H^1_D(\Omega,\mathbb{R}^d)$ *be the adjoint state defined as the weak solution to problem* (4.11)*. Then*

$$J^\varepsilon_{\boldsymbol{u}'}(\boldsymbol{u},\boldsymbol{\varphi})\boldsymbol{u}^* = -\langle\mathcal{E}(\boldsymbol{p}),\mathcal{E}(\boldsymbol{u})\rangle_{\mathbb{C}'(\boldsymbol{\varphi})\boldsymbol{h}} - \int_\Omega h^N\boldsymbol{f}\cdot\boldsymbol{p}. \tag{4.14}$$

Proof. Testing (4.12) with $\boldsymbol{u}^*\in H^1_D(\Omega,\mathbb{R}^d)$ and using (4.5) gives

$$J^\varepsilon_{\boldsymbol{u}'}(\boldsymbol{u},\boldsymbol{\varphi})\boldsymbol{u}^* = \langle\mathcal{E}(\boldsymbol{u}^*),\mathcal{E}(\boldsymbol{p})\rangle_{\mathbb{C}(\boldsymbol{\varphi})}.$$

Using (3.10) with $\boldsymbol{\eta}:=\boldsymbol{p}$ we end up with (4.14). □

Theorem 4.5. *Let* $\boldsymbol{\varphi}\in\boldsymbol{\mathcal{G}}^{\boldsymbol{m}}\cap\boldsymbol{U}_c$ *be a solution to* (4.13)*. Then the following variational inequality is fulfilled:*

$$j'(\boldsymbol{\varphi})(\tilde{\boldsymbol{\varphi}}-\boldsymbol{\varphi})\geq 0 \qquad \forall\tilde{\boldsymbol{\varphi}}\in\boldsymbol{\mathcal{G}}^{\boldsymbol{m}}\cap\boldsymbol{U}_c, \tag{4.15}$$

where

$$\begin{aligned} j'(\boldsymbol{\varphi})(\tilde{\boldsymbol{\varphi}}-\boldsymbol{\varphi}) = J^\varepsilon_{\boldsymbol{\varphi}'}(\boldsymbol{u},\boldsymbol{\varphi})(\tilde{\boldsymbol{\varphi}}-\boldsymbol{\varphi}) - \langle\mathcal{E}(\boldsymbol{p}),\mathcal{E}(\boldsymbol{u})\rangle_{\mathbb{C}'(\boldsymbol{\varphi})(\tilde{\boldsymbol{\varphi}}-\boldsymbol{\varphi})} \\ -\int_\Omega(\tilde{\varphi}^N-\varphi^N)\boldsymbol{f}\cdot\boldsymbol{p}. \end{aligned}$$

Proof. Since $\boldsymbol{\mathcal{G}}^{\boldsymbol{m}}\cap\boldsymbol{U}_c$ is convex, the assertion follows directly. □

We can now state the complete optimality system.

https://doi.org/10.1051/cocv/2014006 Published online by Cambridge University Press

Theorem 4.6. *Let $\boldsymbol{\varphi} \in \boldsymbol{\mathcal{G}}^{\boldsymbol{m}} \cap \boldsymbol{U}_c$ denote a minimizer of the problem $(\mathcal{P}^\varepsilon)$ and $S(\boldsymbol{\varphi}) = \boldsymbol{u} \in H^1_D(\Omega, \mathbb{R}^d)$, $\boldsymbol{p} \in H^1_D(\Omega, \mathbb{R}^d)$ are the corresponding state and adjoint variables, respectively. Then the functions $(\boldsymbol{u}, \boldsymbol{\varphi}, \boldsymbol{p}) \in H^1_D(\Omega, \mathbb{R}^d) \times (\boldsymbol{\mathcal{G}}^{\boldsymbol{m}} \cap \boldsymbol{U}_c) \times H^1_D(\Omega, \mathbb{R}^d)$ fulfill the following optimality system in a weak sense. We obtain the state equations* (SE)

$$\text{(SE)} \quad \begin{cases} -\nabla \cdot [\mathbb{C}(\boldsymbol{\varphi})\mathcal{E}(\boldsymbol{u})] = \left(1-\varphi^N\right)\boldsymbol{f} & \text{in } \Omega, \\ \boldsymbol{u} = \boldsymbol{0} & \text{on } \Gamma_D, \\ [\mathbb{C}(\boldsymbol{\varphi})\mathcal{E}(\boldsymbol{u})]\,\boldsymbol{n} = \boldsymbol{g} & \text{on } \Gamma_g, \\ [\mathbb{C}(\boldsymbol{\varphi})\mathcal{E}(\boldsymbol{u})]\,\boldsymbol{n} = \boldsymbol{0} & \text{on } \Gamma_0, \end{cases}$$

the adjoint equations (AE)

$$\text{(AE)} \quad \begin{cases} -\nabla \cdot [\mathbb{C}(\boldsymbol{\varphi})\mathcal{E}(\boldsymbol{p})] = \alpha\left(1-\varphi^N\right)\boldsymbol{f} \\ \qquad\qquad +2\beta\nu J_0(\boldsymbol{u},\boldsymbol{\varphi})^{\frac{\nu-1}{\nu}} c(1-\varphi^N)(\boldsymbol{u}-\boldsymbol{u}_\Omega) & \text{in } \Omega, \\ \boldsymbol{p} = \boldsymbol{0} & \text{on } \Gamma_D, \\ [\mathbb{C}(\boldsymbol{\varphi})\mathcal{E}(\boldsymbol{p})]\,\boldsymbol{n} = \alpha\boldsymbol{g} & \text{on } \Gamma_g, \\ [\mathbb{C}(\boldsymbol{\varphi})\mathcal{E}(\boldsymbol{p})]\,\boldsymbol{n} = \boldsymbol{0} & \text{on } \Gamma_0 \end{cases}$$

and the gradient inequality (GI)

$$\text{(GI)} \quad \begin{cases} \gamma\varepsilon \int_\Omega \nabla\boldsymbol{\varphi} : \nabla(\tilde{\boldsymbol{\varphi}} - \boldsymbol{\varphi}) + \frac{\gamma}{\varepsilon}\int_\Omega \Psi_0'(\boldsymbol{\varphi})\cdot(\tilde{\boldsymbol{\varphi}} - \boldsymbol{\varphi}) \\ -\beta\nu J_0(\boldsymbol{u},\boldsymbol{\varphi})^{\frac{\nu-1}{\nu}} \int_\Omega c(\tilde{\varphi}^N - \varphi^N)|\boldsymbol{u}-\boldsymbol{u}_\Omega|^2 \\ -\int_\Omega (\tilde{\varphi}^N - \varphi^N)\boldsymbol{f}\cdot(\alpha\boldsymbol{u}+\boldsymbol{p}) - \langle \mathcal{E}(\boldsymbol{p}), \mathcal{E}(\boldsymbol{u})\rangle_{\mathbb{C}'(\boldsymbol{\varphi})(\tilde{\boldsymbol{\varphi}}-\boldsymbol{\varphi})} \geq 0, \\ \forall \tilde{\boldsymbol{\varphi}} \in \boldsymbol{\mathcal{G}}^{\boldsymbol{m}} \cap \boldsymbol{U}_c. \end{cases}$$

Proof. The claim follows directly from Theorem 4.5. □

Remark 4.7. In the case $\beta = 0$ we get $\boldsymbol{p} = \alpha\boldsymbol{u}$ and the first-order optimality system can be written without the adjoint state as follows

$$(\text{SE})_M \quad \begin{cases} -\nabla \cdot [\mathbb{C}(\boldsymbol{\varphi})\mathcal{E}(\boldsymbol{u})] = \left(1-\varphi^N\right)\boldsymbol{f} & \text{in } \Omega, \\ \boldsymbol{u} = \boldsymbol{0} & \text{on } \Gamma_D, \\ [\mathbb{C}(\boldsymbol{\varphi})\mathcal{E}(\boldsymbol{u})]\,\boldsymbol{n} = \boldsymbol{g} & \text{on } \Gamma_g, \\ [\mathbb{C}(\boldsymbol{\varphi})\mathcal{E}(\boldsymbol{u})]\,\boldsymbol{n} = \boldsymbol{0} & \text{on } \Gamma_0, \end{cases}$$

together with

$$(\text{GI})_M \quad \begin{cases} \gamma\varepsilon \int_\Omega \nabla\boldsymbol{\varphi} : \nabla(\tilde{\boldsymbol{\varphi}} - \boldsymbol{\varphi}) + \frac{\gamma}{\varepsilon}\int_\Omega \Psi_0'(\boldsymbol{\varphi})(\tilde{\boldsymbol{\varphi}} - \boldsymbol{\varphi}) \\ -2\alpha \int_\Omega (\tilde{\varphi}^N - \varphi^N)\boldsymbol{f}\cdot\boldsymbol{u} - \alpha\langle \mathcal{E}(\boldsymbol{u}), \mathcal{E}(\boldsymbol{u})\rangle_{\mathbb{C}'(\boldsymbol{\varphi})(\tilde{\boldsymbol{\varphi}}-\boldsymbol{\varphi})} \geq 0, \\ \forall \tilde{\boldsymbol{\varphi}} \in \boldsymbol{\mathcal{G}}^{\boldsymbol{m}} \cap \boldsymbol{U}_c. \end{cases}$$

https://doi.org/10.1051/cocv/2014006 Published online by Cambridge University Press

5. Sharp interface asymptotics

In this section we derive the sharp interface limit of the optimality system derived in Theorem 4.6. The discussion in this section will not be rigorous and in particular we will use the method of formally matched asymptotic expansions where asymptotic expansions in bulk regions have to be matched with expansions in interfacial regions.

For solutions $(\boldsymbol{u}^\varepsilon, \boldsymbol{\varphi}^\varepsilon, \boldsymbol{p}^\varepsilon)$ of the optimality system in Theorem 4.6 we perform formally matched asymptotic expansions. It will turn out that the phase field $\boldsymbol{\varphi}^\varepsilon$ will change its values rapidly on a length scale proportional to ε. For additional information on asymptotic expansions for phase field equations we refer to [1,27]. From now on we will assume that $\mathbb{C}(\boldsymbol{\varphi})$ has the form in (2.10) and that the functions c and $\boldsymbol{u}_\Omega$ in the compliant mechanism functional J_0 are smooth functions. In what follows we need to introduce Lagrange multipliers $\boldsymbol{\lambda} = (\lambda^i)_{i=1}^N$ with $\sum_{i=1}^N \lambda^i = 0$ for the integral constraint $\fint_\Omega \boldsymbol{\varphi} = \boldsymbol{m}$, see [8,49,65]. Then the gradient inequality (GI) in Theorem 4.6 can be reformulated as

$$
\text{(GI')}\quad \begin{cases} \gamma\varepsilon \int_\Omega \nabla\boldsymbol{\varphi} : \nabla(\tilde{\boldsymbol{\varphi}} - \boldsymbol{\varphi}) + \frac{\gamma}{\varepsilon} \int_\Omega \Psi_0'(\boldsymbol{\varphi}) \cdot (\tilde{\boldsymbol{\varphi}} - \boldsymbol{\varphi}) \\ -\beta\nu J_0(\boldsymbol{u}, \boldsymbol{\varphi})^{\frac{\nu-1}{\nu}} \int_\Omega c(\tilde{\varphi}^N - \varphi^N)|\boldsymbol{u} - \boldsymbol{u}_\Omega|^2 \\ -\int_\Omega (\tilde{\varphi}^N - \varphi^N)\boldsymbol{f} \cdot (\alpha\boldsymbol{u} + \boldsymbol{p}) - \langle \mathcal{E}(\boldsymbol{p}), \mathcal{E}(\boldsymbol{u})\rangle_{\mathbb{C}'(\boldsymbol{\varphi})(\tilde{\boldsymbol{\varphi}} - \boldsymbol{\varphi})} \\ +\int_\Omega \boldsymbol{\lambda} \cdot (\tilde{\boldsymbol{\varphi}} - \boldsymbol{\varphi}) \geq 0, \\ \forall \tilde{\boldsymbol{\varphi}} \in \boldsymbol{\mathcal{G}} \cap \boldsymbol{U}_c. \end{cases}
$$

5.1. Outer expansions (expansion in bulk regions)

We first expand the solution in outer regions away from the interface. We assume an expansion of the form $\boldsymbol{u}^\varepsilon(x) = \sum_{k=0}^\infty \varepsilon^k \boldsymbol{u}_k(x)$, $\boldsymbol{p}^\varepsilon(x) = \sum_{k=0}^\infty \varepsilon^k \boldsymbol{p}_k(x)$, $\boldsymbol{\varphi}^\varepsilon(x) = \sum_{k=0}^\infty \varepsilon^k \boldsymbol{\varphi}_k(x)$, where $\boldsymbol{\varphi}_0(x) \in \boldsymbol{G}$, $\fint_\Omega \boldsymbol{\varphi}_0 = \boldsymbol{m}$, $\boldsymbol{\varphi}_k(x) \in T\Sigma^N$, $\fint_\Omega \boldsymbol{\varphi}_k = 0$ for $k \geq 1$, $\boldsymbol{\varphi}_0 \in \boldsymbol{U}_c$ and $\boldsymbol{\varphi}_k = \boldsymbol{0}$ on $S_0 \cup S_1$ for $k \geq 1$. Since the Ψ-term in the energy (2.1) scales with $\frac{1}{\varepsilon}$ we obtain

$$
\int_\Omega \Psi(\boldsymbol{\varphi}_0) = 0,
$$

which follows by arguments similar as in [4], Theorem 2.5. Hence, $\Psi(\boldsymbol{\varphi}_0) = 0$ a.e. in Ω and we obtain that $\boldsymbol{\varphi}_0$ has to attain the values $\boldsymbol{e}_1, \ldots, \boldsymbol{e}_N$ which are the N global minima of Ψ with height 0. Hence, to leading order the domain Ω is partitioned into N regions $\Omega^i, i \in \{1, \ldots, N\}$, where $\boldsymbol{\varphi}_0 = \boldsymbol{e}_i, i \in \{1, \ldots, N\}$. In the regions Ω^i, $i = 1, \ldots, N-1$, we observe by using a Taylor expansion in $\mathbb{C}(\boldsymbol{\varphi}^\varepsilon)$ that up to terms of order ε the following identity holds $\mathbb{C}(\boldsymbol{\varphi}_0) = \mathbb{C}(\boldsymbol{e}_i) = \mathbb{C}^i$, see also Section 2.2. This now makes it straightforward to obtain the leading order expansion of the state and adjoint equations in the regions Ω^i, $i = 1, \ldots, N-1$. Choosing $\boldsymbol{u} = \boldsymbol{u}^\varepsilon$ and $\boldsymbol{\varphi} = \boldsymbol{\varphi}^\varepsilon$ in the state equation (2.4) we obtain *e.g.* to leading order ε^0 in the first equation of (2.4):

$$
-\nabla \cdot [\mathbb{C}(\boldsymbol{\varphi}_0)\mathcal{E}(\boldsymbol{u}_0)] = \boldsymbol{f} \text{ in } \Omega^i
$$

and on $\Gamma_g \cap \partial\Omega^i$ we obtain to leading order

$$
[\mathbb{C}(\boldsymbol{\varphi}_0)\mathcal{E}(\boldsymbol{p}_0)]\,\boldsymbol{n} = \alpha\boldsymbol{g} \text{ on } \Gamma_g \cap \partial\Omega^i.
$$

https://doi.org/10.1051/cocv/2014006 Published online by Cambridge University Press

All other terms in the state equation (2.4) and in the adjoint equation (4.11) can be treated similarly and altogether we obtain for $i \in \{1, \dots, N-1\}$

$$(\mathrm{SE})^i \begin{cases} -\nabla \cdot \left[\mathbb{C}^i \mathcal{E}(\boldsymbol{u}_0)\right] = \boldsymbol{f} & \text{in } \Omega^i, \\ \boldsymbol{u}_0 = \boldsymbol{0} & \text{on } \Gamma_D \cap \partial\Omega^i, \\ \left[\mathbb{C}^i \mathcal{E}(\boldsymbol{u}_0)\right] \boldsymbol{n} = \boldsymbol{g} & \text{on } \Gamma_g \cap \partial\Omega^i, \\ \left[\mathbb{C}^i \mathcal{E}(\boldsymbol{u}_0)\right] \boldsymbol{n} = \boldsymbol{0} & \text{on } \Gamma_0 \cap \partial\Omega^i, \end{cases}$$

$$(\mathrm{AE})^i \begin{cases} -\nabla \cdot \left[\mathbb{C}^i \mathcal{E}(\boldsymbol{p}_0)\right] = \alpha \boldsymbol{f} + 2\beta\nu J_0(\boldsymbol{u}, \boldsymbol{\varphi})^{\frac{\nu-1}{\nu}} c(\boldsymbol{u}_0 - \boldsymbol{u}_\Omega) & \text{in } \Omega^i, \\ \boldsymbol{p}_0 = \boldsymbol{0} & \text{on } \Gamma_D \cap \partial\Omega^i, \\ \left[\mathbb{C}^i \mathcal{E}(\boldsymbol{p}_0)\right] \boldsymbol{n} = \alpha \boldsymbol{g} & \text{on } \Gamma_g \cap \partial\Omega^i, \\ \left[\mathbb{C}^i \mathcal{E}(\boldsymbol{p}_0)\right] \boldsymbol{n} = \boldsymbol{0} & \text{on } \Gamma_0 \cap \partial\Omega^i. \end{cases}$$

In the domain Ω^N the elasticity tensor $\mathbb{C}^N$ converges to zero, see Section 2.2, and we obtain no relevant equation to leading order.

5.2. Inner expansions

We now construct a solution in the interfacial regions.

5.2.1. New coordinates in the inner region

Denoting by Γ_{ij} a smooth interface separating Ω^i and Ω^j which we expect to obtain in the limit when ε tends to zero, we now introduce new coordinates in a neighborhood of Γ_{ij}. To keep the notation simple we sometimes denote Γ_{ij} by Γ. Choosing a spatial parameter domain $U \subset \mathbb{R}^{d-1}$ we define a local parametrization

$$\boldsymbol{\gamma} : U \to \mathbb{R}^d$$

of Γ. By $\boldsymbol{\nu}$ we denote the unit normal to Γ pointing from Ω^i to Ω^j.

Close to $\boldsymbol{\gamma}(U)$ we consider the signed distance function $d(x)$ of a point x to Γ with $d(x) > 0$ if $x \in \Omega^j$. We introduce a local parametrization of $\mathbb{R}^d$ close to $\boldsymbol{\gamma}(U)$ using the rescaled distance $z = \frac{d}{\varepsilon}$ as follows

$$G^\varepsilon(s, z) := \boldsymbol{\gamma}(s) + \varepsilon z \boldsymbol{\nu}(s),$$

where $s \in U \subset \mathbb{R}^{d-1}$. Let $(s_1, \dots, s_{d-1}) \in U$. Then

$$\partial_{s_1}\boldsymbol{\gamma} + \varepsilon z \partial_{s_1}\boldsymbol{\nu}, \dots, \partial_{s_{d-1}}\boldsymbol{\gamma} + \varepsilon z \partial_{s_{d-1}}\boldsymbol{\nu}, \, \varepsilon\boldsymbol{\nu}$$

is a basis of $\mathbb{R}^d$ locally around Γ. We refer to Figure 1 for an illustration of the geometry around the interface Γ_{ij}.

Denoting by s_d the z-variable we have for a scalar function $b(x) = \hat{b}(z(x), s(x))$

$$\nabla_x b = \nabla_{\Gamma_{\varepsilon z}} \hat{b} + \tfrac{1}{\varepsilon} \partial_z \hat{b} \, \boldsymbol{\nu}. \tag{5.1}$$

Here $\nabla_{\Gamma_{\varepsilon z}} \hat{b}$ is the surface gradient $\nabla_{\Gamma_{\varepsilon z}} b_{|\Gamma_{\varepsilon z}}$ on $\Gamma_{\varepsilon z} := \{\boldsymbol{\gamma}(s) + \varepsilon z \boldsymbol{\nu}(s) \mid s \in U\}$. In addition we compute for a vector quantity $\mathbf{j}(x) = \hat{\mathbf{j}}(z(x), s(x))$

$$\nabla_x \cdot \mathbf{j} = \nabla_{\Gamma_{\varepsilon z}} \cdot \hat{\mathbf{j}} + \tfrac{1}{\varepsilon} \partial_z \hat{\mathbf{j}} \cdot \boldsymbol{\nu}, \tag{5.2}$$

where $\nabla_{\Gamma_{\varepsilon z}} \cdot \hat{\mathbf{j}}$ is the divergence on $\Gamma_{\varepsilon z}$. We also compute

$$\Delta_x b = \Delta_{\Gamma_{\varepsilon z}} \hat{b} + \tfrac{1}{\varepsilon} (\Delta_x d) \partial_z \hat{b} + \tfrac{1}{\varepsilon^2} \partial_{zz} \hat{b}$$

https://doi.org/10.1051/cocv/2014006 Published online by Cambridge University Press

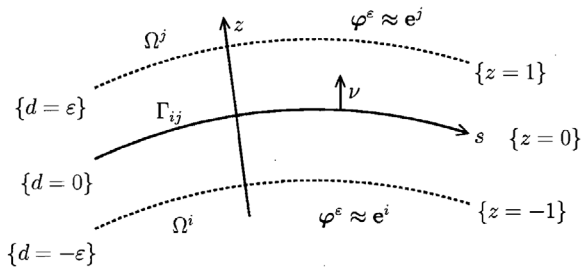


FIGURE 1. The geometry close to the interface Γ_{ij}.

and derive

$$\nabla_{\Gamma_{\varepsilon z}} \hat{b}(z,s) = \nabla_\Gamma \hat{b}(z,s) + \text{ h.o.t.},$$
$$\nabla_{\Gamma_{\varepsilon z}} \cdot \hat{\mathbf{j}}(z,s) = \nabla_\Gamma \cdot \hat{\mathbf{j}}(z,s) + \text{ h.o.t.},$$
$$\Delta_{\Gamma_{\varepsilon z}} \hat{b}(z,s) = \Delta_\Gamma \hat{b}(z,s) + \text{ h.o.t.},$$

where ∇_Γ, $\nabla_\Gamma\cdot$ and Δ_Γ are computed on $\Gamma_{\varepsilon z}$ with the metric tensor on Γ and h.o.t. stands for higher order terms in ε, see [1]. We denote by κ the mean curvature which is defined to be the sum of the principal curvatures $\kappa_1, \ldots, \kappa_{d-1}$. We choose the sign convention that κ is positive when the surface is curved in the direction of the normal $\boldsymbol{\nu}$. By $|\mathcal{S}|$ we denote the spectral norm of the Weingarten map $\mathcal{S}$ and hence $|\mathcal{S}| = \kappa_1^2 + \ldots + \kappa_{d-1}^2$. We now obtain as in [1]

$$\Delta_x b = \Delta_\Gamma \hat{b} - \tfrac{1}{\varepsilon}(\kappa + \varepsilon z|\mathcal{S}|^2)\partial_z \hat{b} + \tfrac{1}{\varepsilon^2}\partial_{zz}\hat{b} + \text{ h.o.t.}.$$

Now using (5.1) we have for a vector quantity $\boldsymbol{b}(x) = \hat{\boldsymbol{b}}(z(x), s(x))$

$$\nabla_x \boldsymbol{b} = \nabla_\Gamma \hat{\boldsymbol{b}} + \tfrac{1}{\varepsilon}\partial_z \hat{\boldsymbol{b}} \otimes \boldsymbol{\nu} + \text{h.o.t.}. \tag{5.3}$$

Furthermore, for a second order tensor quantity $\mathcal{A}(x) = (a_{\mathrm{ij}}(x))_{i,j=1}^d = \hat{\mathcal{A}}(z(x), s(x))$ with $\mathcal{A} = (\boldsymbol{j}_i)_{i=1}^d$, where $\boldsymbol{j}_i = (a_{\mathrm{ij}})_{j=1}^d$, the divergence is defined by $\nabla_x \cdot \mathcal{A} = (\nabla_x \cdot \boldsymbol{j}_i)_{i=1}^d$ and by (5.2) we get

$$\nabla_x \cdot \mathcal{A} = \nabla_\Gamma \cdot \hat{\mathcal{A}} + \frac{1}{\varepsilon}\partial_z \hat{\mathcal{A}}\,\boldsymbol{\nu} + \text{h.o.t.}. \tag{5.4}$$

For the inner expansion we make the ansatz

$$\boldsymbol{U}^\varepsilon(x) = \sum_{k=0}^{\infty} \varepsilon^k \boldsymbol{U}_k(z(x), s(x)), \tag{5.5}$$

$$\boldsymbol{P}^\varepsilon(x) = \sum_{k=0}^{\infty} \varepsilon^k \boldsymbol{P}_k(z(x), s(x)), \tag{5.6}$$

$$\boldsymbol{\Phi}^\varepsilon(x) = \sum_{k=0}^{\infty} \varepsilon^k \boldsymbol{\Phi}_k(z(x), s(x)), \tag{5.7}$$

where $\boldsymbol{\Phi}_0(z(x), s(x)) \in \Sigma^N$, $\boldsymbol{\Phi}_k(z(x), s(x)) \in T\Sigma^N$, $\forall k \geq 1$. We remark that no interface occurs on $S_0 \cup S_1$ as we set $\varphi^N = 0$ on S_0 and $\varphi^N = 1$ on S_1.

https://doi.org/10.1051/cocv/2014006 Published online by Cambridge University Press

5.2.2. Matching conditions

The outer expansions hold in the regions Ω^i, $i = 1, \dots, N$, and the inner expansions are supposed to hold in a tubular neighborhood around Γ_{ij} which is scaled by ε. These two approximations are assumed to hold simultaneously in a suitable region close to Γ_{ij} which is given by points x with the property $\mathrm{dist}(x, \Gamma) \approx \varepsilon^\theta$, $0 < \theta < 1$. Comparing the two expansions in the intermediate region leads to matching conditions which relate the outer expansions to the inner expansions *via* boundary conditions for the outer expansions which are expressed with the help of the inner variables, see [26,27,35] for details. Indeed, we need the following matching conditions at $x = \boldsymbol{\gamma}(s)$:

$$\boldsymbol{\Phi}_0(z,s) \to \begin{cases} (\boldsymbol{\varphi}_0)_j = \boldsymbol{e}_j & \text{for} \quad z \to +\infty, \\ (\boldsymbol{\varphi}_0)_i = \boldsymbol{e}_i & \text{for} \quad z \to -\infty, \end{cases} \tag{5.8}$$

$$\partial_z \boldsymbol{\Phi}_1(z,s) \to \begin{cases} (\nabla \boldsymbol{\varphi}_0)_j \boldsymbol{\nu} & \text{for} \quad z \to +\infty, \\ (\nabla \boldsymbol{\varphi}_0)_i \boldsymbol{\nu} & \text{for} \quad z \to -\infty, \end{cases} \tag{5.9}$$

where for a quantity $(\boldsymbol{v})_j := \lim\limits_{\delta \searrow 0} \boldsymbol{v}(x + \delta \boldsymbol{\nu})$ and $(\boldsymbol{v})_i := \lim\limits_{\delta \searrow 0} \boldsymbol{v}(x - \delta \boldsymbol{\nu})$ for $x \in \Gamma$. We remark that for $\delta > 0$ small we have $x + \delta \boldsymbol{\nu} \in \Omega^j$ and $x - \delta \boldsymbol{\nu} \in \Omega^i$. In addition we obtain that if

$$\boldsymbol{\Phi}_1(z,s) = \begin{cases} \boldsymbol{A}_j(s) + \boldsymbol{B}_j(s) z + \boldsymbol{o}(1) & \text{for} \quad z \to +\infty, \\ \boldsymbol{A}_i(s) + \boldsymbol{B}_i(s) z + \boldsymbol{o}(1) & \text{for} \quad z \to -\infty, \end{cases}$$

the identities

$$\boldsymbol{A}_j(s) = (\boldsymbol{\varphi}_1)_j, \quad \boldsymbol{A}_i(s) = (\boldsymbol{\varphi}_1)_i, \tag{5.10}$$

$$\boldsymbol{B}_j(s) = (\nabla \boldsymbol{\varphi}_0)_j \boldsymbol{\nu}, \quad \boldsymbol{B}_i(s) = (\nabla \boldsymbol{\varphi}_0)_i \boldsymbol{\nu} \tag{5.11}$$

have to hold, see [26,35]. Of course similar relations hold for the other functions like $\boldsymbol{u}$ and $\boldsymbol{p}$. In the following we will use for a quantity $\boldsymbol{v}$ the jump across the interface Γ which is denoted by $[\boldsymbol{v}]_i^j$ and defined as

$$[\boldsymbol{v}]_i^j := \lim_{\delta \searrow 0} \left(\boldsymbol{v}(x + \delta \boldsymbol{\nu}) - \boldsymbol{v}(x - \delta \boldsymbol{\nu}) \right) \text{ for } x \in \Gamma.$$

5.2.3. The equations to leading order

Plugging the asymptotic expansions into the optimality system in Theorem 4.6 we ask that each individual coefficient of a power in ε vanishes. For the state equation using (5.1), (5.4) and $\partial_z \boldsymbol{\nu} = \boldsymbol{0}$ we compute

$$\begin{aligned} -\nabla_x \cdot [\mathbb{C}(\boldsymbol{\varphi}) \mathcal{E}(\boldsymbol{u})] = & -\frac{1}{\varepsilon^2} \partial_z [\mathbb{C}(\boldsymbol{\Phi})(\partial_z \boldsymbol{U} \otimes \boldsymbol{\nu})^{\mathrm{sym}} \boldsymbol{\nu}] - \frac{1}{\varepsilon} \partial_z \left[\mathbb{C}(\boldsymbol{\Phi})(\nabla_{\Gamma_{\varepsilon z}} \boldsymbol{U})^{\mathrm{sym}} \boldsymbol{\nu} \right] \\ & - \frac{1}{\varepsilon} \nabla_{\Gamma_{\varepsilon z}} \cdot [\mathbb{C}(\boldsymbol{\Phi})(\partial_z \boldsymbol{U} \otimes \boldsymbol{\nu})^{\mathrm{sym}}] - \nabla_{\Gamma_{\varepsilon z}} \cdot [\mathbb{C}(\boldsymbol{\Phi})(\nabla_{\Gamma_{\varepsilon z}} \boldsymbol{U})^{\mathrm{sym}}]. \end{aligned}$$

We obtain to leading order $\mathcal{O}\left(\frac{1}{\varepsilon^2}\right)$:

$$\partial_z \left[\overline{\mathbb{C}}(\boldsymbol{\Phi}_0)(\partial_z \boldsymbol{U}_0 \otimes \boldsymbol{\nu})^{\mathrm{sym}} \boldsymbol{\nu} \right] = \boldsymbol{0}. \tag{5.12}$$

Multiplying (5.12) by $\boldsymbol{U}_0$, integrating over $z \in (-\infty, +\infty)$ we obtain using integration by parts and $\lim\limits_{z \to \pm\infty} \partial_z \boldsymbol{U}_0(z) = \boldsymbol{0}$ (using the matching conditions)

$$0 = \int_{-\infty}^{+\infty} \overline{\mathbb{C}}(\boldsymbol{\Phi}_0)(\partial_z \boldsymbol{U}_0 \otimes \boldsymbol{\nu})^{\mathrm{sym}} : (\partial_z \boldsymbol{U}_0 \otimes \boldsymbol{\nu})^{\mathrm{sym}} \mathrm{d}z.$$

https://doi.org/10.1051/cocv/2014006 Published online by Cambridge University Press

We obtain $(\partial_z \boldsymbol{U}_0 \otimes \boldsymbol{\nu})^{\mathrm{sym}} = 0$ which gives that $\boldsymbol{U}_0$ is constant in z. This implies after matching for $i, j \neq N$

$$[\boldsymbol{u}_0]_i^j = \boldsymbol{0}.$$

Similarly for the adjoint equation we obtain to leading order $\mathcal{O}\left(\frac{1}{\varepsilon^2}\right)$ that $\boldsymbol{P}_0$ is constant in z and for $i, j \neq N$

$$[\boldsymbol{p}_0]_i^j = \boldsymbol{0}.$$

We now want to analyze the state and the adjoint equation to the next order $\mathcal{O}\left(\frac{1}{\varepsilon}\right)$. Using the representation of ∇_x and $\nabla_x \cdot$ in the new coordinates, see (5.1) and (5.2), we obtain

$$\begin{aligned} \nabla_x \cdot (\nabla_x \boldsymbol{u}) &= \nabla_x \cdot (\nabla_\Gamma \boldsymbol{U} + \tfrac{1}{\varepsilon} \partial_z \boldsymbol{U} \otimes \boldsymbol{\nu}) \\ &= \tfrac{1}{\varepsilon} \partial_z (\nabla_\Gamma \boldsymbol{U} + \tfrac{1}{\varepsilon} \partial_z \boldsymbol{U} \otimes \boldsymbol{\nu}) \cdot \boldsymbol{\nu} + \nabla_\Gamma \cdot (\nabla_\Gamma \boldsymbol{U} + \tfrac{1}{\varepsilon} \partial_z \boldsymbol{U} \otimes \boldsymbol{\nu}) \end{aligned} \tag{5.13}$$

Using the expansion (5.5) for $\boldsymbol{U}$, noting the fact that $\partial_z \boldsymbol{U}_0 = \boldsymbol{0}$ and applying a similar argument for the term involving $(\nabla_x \boldsymbol{u})^T$ we derive from the equation $\nabla_x \cdot [\mathbb{C}(\boldsymbol{\varphi}) \mathcal{E}(\boldsymbol{u})] = 0$ to the order $\mathcal{O}\left(\frac{1}{\varepsilon}\right)$:

$$\partial_z [\overline{\mathbb{C}}(\boldsymbol{\Phi}_0)(\partial_z \boldsymbol{U}_1 \otimes \boldsymbol{\nu} + \nabla_\Gamma \boldsymbol{U}_0)^{\mathrm{sym}} \boldsymbol{\nu}] = \boldsymbol{0}. \tag{5.14}$$

Matching requires

$$\partial_z \boldsymbol{U}_1 \otimes \boldsymbol{\nu} + \nabla_\Gamma \boldsymbol{U}_0 \to \begin{cases} (\nabla_x \boldsymbol{u}_0)_j & \text{for} \quad z \to +\infty, \\ (\nabla_x \boldsymbol{u}_0)_i & \text{for} \quad z \to -\infty. \end{cases} \tag{5.15}$$

Hence (5.14) and (5.15) give for $i \neq N$

$$\mathbb{C}^i \mathcal{E}_i(\boldsymbol{u}_0) \boldsymbol{\nu} = \begin{cases} \boldsymbol{0} & \text{if} \quad j = N, \\ \mathbb{C}^j \mathcal{E}_j(\boldsymbol{u}_0) \boldsymbol{\nu} & \text{if} \quad j \neq N, \end{cases}$$

where $\mathcal{E}_i(\boldsymbol{u}_0) := \lim\limits_{\delta \searrow 0} \mathcal{E}(\boldsymbol{u}_0)(x - \delta \boldsymbol{\nu})$ and $\mathcal{E}_j(\boldsymbol{u}_0) := \lim\limits_{\delta \searrow 0} \mathcal{E}(\boldsymbol{u}_0)(x + \delta \boldsymbol{\nu})$.

A similar reasoning provides for $i \neq N$

$$\mathbb{C}^i \mathcal{E}_i(\boldsymbol{p}_0) \boldsymbol{\nu} = \begin{cases} \boldsymbol{0} & \text{if} \quad j = N, \\ \mathbb{C}^j \mathcal{E}_j(\boldsymbol{p}_0) \boldsymbol{\nu} & \text{if} \quad j \neq N. \end{cases}$$

In order to deal with the sum constraint $\sum\limits_{i=1}^N \varphi^i = 1$ we introduce an orthogonal projection, see [8]:

$$\boldsymbol{P}_{T\Sigma} : \mathbb{R}^N \to T\Sigma^N, \quad \boldsymbol{P}_{T\Sigma} \boldsymbol{\varphi} = \boldsymbol{\varphi} - \left(\frac{1}{N} \sum_{i=1}^N \varphi^i \right) \boldsymbol{1},$$

where $\boldsymbol{1} := (1, \ldots, 1)^T$. As the gradient inequality results in an equation in the interior of the Gibbs simplex using (GI') we obtain, see also [5], to leading order $\mathcal{O}\left(\frac{1}{\varepsilon}\right)$:

$$\boldsymbol{\lambda}_0 = \gamma \partial_{zz} \boldsymbol{\Phi}_0 - \gamma \boldsymbol{P}_{T\Sigma} \Psi_0'(\boldsymbol{\Phi}_0), \tag{5.16}$$

where $\boldsymbol{\lambda}_0 + \varepsilon \boldsymbol{\lambda}_1 + \ldots$ is the inner expansion of the Lagrange multiplier variable $\boldsymbol{\lambda}_\varepsilon$. We multiply (5.16) with $\partial_z \boldsymbol{\Phi}_0$, integrate with respect to z, use (5.8) and $\Psi(\boldsymbol{e}_i) = 0$, $i \in \{1, \ldots, N\}$ and obtain $\boldsymbol{\lambda}_0 \cdot (\boldsymbol{e}_j - \boldsymbol{e}_i) = 0$. Using $\sum\limits_{i=1}^N \lambda_0^i = 0$ we get

$$\boldsymbol{\lambda}_0 = \boldsymbol{0}. \tag{5.17}$$

https://doi.org/10.1051/cocv/2014006 Published online by Cambridge University Press

Now $\boldsymbol{\Phi}_0$ is obtained as a solution of

$$\mathbf{0} = \partial_{zz}\boldsymbol{\Phi}_0 - \boldsymbol{P}_{T\Sigma}\Psi_0'(\boldsymbol{\Phi}_0), \tag{5.18}$$

connecting the values $\boldsymbol{e}_i$ and $\boldsymbol{e}_j$, see [13].

Furthermore in the interior of the Gibbs simplex using (GI') we obtain to the order $\mathcal{O}(1)$:

$$\begin{aligned}
&\frac{1}{\gamma}\boldsymbol{\lambda}_1 + \partial_{zz}\boldsymbol{\Phi}_1 - \boldsymbol{P}_{T\Sigma}\Psi_0''(\boldsymbol{\Phi}_0)\boldsymbol{\Phi}_1 \\
&\quad = \kappa\partial_z\boldsymbol{\Phi}_0 - \frac{\beta\nu J_0(\boldsymbol{u}_0,\boldsymbol{\varphi}_0)^{\frac{\nu-1}{\nu}}}{\gamma}c|\boldsymbol{U}_0 - \boldsymbol{u}_\Omega|^2\boldsymbol{e}_N - \frac{1}{\gamma}\boldsymbol{f}\cdot(\alpha\boldsymbol{U}_0 + \boldsymbol{P}_0)\boldsymbol{e}_N \\
&\qquad - \frac{1}{\gamma}[\overline{\mathbb{C}}'(\boldsymbol{\Phi}_0)(\partial_z\boldsymbol{U}_1\otimes\boldsymbol{\nu} + \nabla_\Gamma\boldsymbol{U}_0)^{\mathrm{sym}} : (\partial_z\boldsymbol{P}_1\otimes\boldsymbol{\nu} + \nabla_\Gamma\boldsymbol{P}_0)^{\mathrm{sym}}].
\end{aligned} \tag{5.19}$$

In order to be able to obtain a solution $\boldsymbol{\Phi}_1$ from (5.19) a solvability condition has to hold. This solvability condition will yield a gradient equation in the sharp interface situation. We multiply (5.19) with $\partial_z\boldsymbol{\Phi}_0$, integrate with respect to z, use $\partial_z\boldsymbol{\nu} = \mathbf{0}$, (5.14) and obtain after integration by parts

$$\begin{aligned}
&\frac{1}{\gamma}\boldsymbol{\lambda}_1\cdot(\boldsymbol{e}_j - \boldsymbol{e}_i) + \int_{-\infty}^{\infty}(\partial_{zz}(\partial_z\boldsymbol{\Phi}_0) - \Psi_0''(\boldsymbol{\Phi}_0)\partial_z\boldsymbol{\Phi}_0)\cdot\boldsymbol{\Phi}_1 \\
&= \sigma_{\mathrm{ij}}\kappa - \frac{\beta\nu J_0(\boldsymbol{u}_0,\boldsymbol{\varphi}_0)^{\frac{\nu-1}{\nu}}}{\gamma}\int_{-\infty}^{\infty} c\,|\boldsymbol{U}_0 - \boldsymbol{u}_\Omega|^2\boldsymbol{e}_N\cdot\partial_z\boldsymbol{\Phi}_0 \\
&\quad - \frac{1}{\gamma}\int_{-\infty}^{\infty}\boldsymbol{f}\cdot(\alpha\boldsymbol{U}_0 + \boldsymbol{P}_0)\boldsymbol{e}_N\cdot\partial_z\boldsymbol{\Phi}_0 \\
&\quad - \frac{1}{\gamma}\int_{-\infty}^{\infty}\frac{\mathrm{d}}{\mathrm{d}z}\left(\overline{\mathbb{C}}(\boldsymbol{\Phi}_0)(\partial_z\boldsymbol{U}_1\otimes\boldsymbol{\nu} + \nabla_\Gamma\boldsymbol{U}_0)^{\mathrm{sym}} : (\partial_z\boldsymbol{P}_1\otimes\boldsymbol{\nu} + \nabla_\Gamma\boldsymbol{P}_0)^{\mathrm{sym}}\right) \\
&\quad + \frac{1}{\gamma}\int_{-\infty}^{\infty}\frac{\mathrm{d}}{\mathrm{d}z}[\overline{\mathbb{C}}(\boldsymbol{\Phi}_0)(\partial_z\boldsymbol{P}_1\otimes\boldsymbol{\nu} + \nabla_\Gamma\boldsymbol{P}_0)^{\mathrm{sym}}\boldsymbol{\nu}\cdot\partial_z\boldsymbol{U}_1]\mathrm{d}z \\
&\quad + \frac{1}{\gamma}\int_{-\infty}^{\infty}\frac{\mathrm{d}}{\mathrm{d}z}[\overline{\mathbb{C}}(\boldsymbol{\Phi}_0)(\partial_z\boldsymbol{U}_1\otimes\boldsymbol{\nu} + \nabla_\Gamma\boldsymbol{U}_0)^{\mathrm{sym}}\boldsymbol{\nu}\cdot\partial_z\boldsymbol{P}_1]\mathrm{d}z,
\end{aligned} \tag{5.20}$$

where $\sigma_{\mathrm{ij}} := \int_{-\infty}^{\infty}|\partial_z\boldsymbol{\Phi}_0|^2\mathrm{d}z$. By virtue of (5.18) we have

$$\sigma_{\mathrm{ij}} = 2\int_{-\infty}^{\infty}\Psi_0(\boldsymbol{\Phi}_0)\mathrm{d}z.$$

Because $\partial_z\boldsymbol{\Phi}_0$ lies in the kernel of $\partial_{zz}\boldsymbol{\Phi}_1 - \Psi_0''(\boldsymbol{\Phi}_0)\boldsymbol{\Phi}_1$, see [26], we obtain

$$\int_{-\infty}^{\infty}(\partial_{zz}(\partial_z\boldsymbol{\Phi}_0) - \Psi_0''(\boldsymbol{\Phi}_0)\partial_z\boldsymbol{\Phi}_0)\cdot\boldsymbol{\Phi}_1 = 0. \tag{5.21}$$

Now we combine (5.20) and (5.21), use the fact that $\boldsymbol{U}_0$ and $\boldsymbol{P}_0$ do not depend on z and then obtain after matching for all $i, j \neq N$

$$0 = \gamma\sigma_{\mathrm{ij}}\kappa - [\mathbb{C}\mathcal{E}(\boldsymbol{u}_0) : \mathcal{E}(\boldsymbol{p}_0)]_i^j + [\mathbb{C}\mathcal{E}(\boldsymbol{u}_0)\boldsymbol{\nu}\cdot(\nabla\boldsymbol{p}_0)\boldsymbol{\nu}]_i^j + [\mathbb{C}\mathcal{E}(\boldsymbol{p}_0)\boldsymbol{\nu}\cdot(\nabla\boldsymbol{u}_0)\boldsymbol{\nu}]_i^j - \lambda_1^j + \lambda_1^i$$

and for all $i \neq N$

$$0 = \gamma\sigma_{\mathrm{iN}}\kappa + \mathbb{C}_i\mathcal{E}_i(\boldsymbol{u}_0) : \mathcal{E}_i(\boldsymbol{p}_0) - \beta\nu J_0(\boldsymbol{u}_0,\boldsymbol{\varphi}_0)^{\frac{\nu-1}{\nu}}c|\boldsymbol{u}_0 - \boldsymbol{u}_\Omega|^2 - \boldsymbol{f}\cdot(\alpha\boldsymbol{u}_0 + \boldsymbol{p}_0) + \lambda_1^i - \lambda_1^N.$$

https://doi.org/10.1051/cocv/2014006 Published online by Cambridge University Press

5.3. Triple junction expansion and matching to the transition layer solutions

In a multi-material structure there are regions occupied by the individual materials (or by void), there are interfacial regions where two materials (or a material and void) meet and finally there are regions where three materials (or two materials and void) meet, see *e.g.* Figure 6. At points where in the sharp interface limit three materials (or two materials and void) meet in addition another condition has to hold. It is well known that in situations where only surface energy is considered an angle condition has to hold at such points. We now want to identify the condition in our setting and are in particular interested to which degree the elasticity equation influences the angle condition. A method to identify the condition at the triple junction which arises from the phase field system in the sharp interface limit, has been introduced by [15], see also [13,33]. In order to do so, one considers an ε-expansion close to the triple junction in rescaled variables which then is plugged into the optimality system in Theorem 4.6. As has been done in [13,15,33] a first order solution only exists if a certain solvability condition holds. In other phase field systems this solvability conditions lead to an angle condition at the triple junction [13,15,33]. The question now arises whether this condition is altered in case that elastic effects are included.

We now construct a solution in the neighborhood of a triple point, where three phases meet, each phase corresponding to one of the three different values $\boldsymbol{e}_j$, $\boldsymbol{e}_k$, $\boldsymbol{e}_l$. We follow the ideas of [13,15,46]. We perform the analysis in $\mathbb{R}^2$ but the method also works in $\mathbb{R}^3$ by using the arguments in the space normal to the triple line, see [13,42]. Assume that $\Gamma^\varepsilon_{\rm jk}, \Gamma^\varepsilon_{\rm kl}, \Gamma^\varepsilon_{\rm lj}$ are three curves that meet at the point $m^\varepsilon_{\rm jkl}$. We use the notation (ab) for any of the three pairs (jk), (kl), (lj). On each $\Gamma^\varepsilon_{\rm ab}$ we choose the normal $\nu^\varepsilon_{\rm ab}$ to point into Ω^b-phase. We introduce the rescaled coordinates $y(x,\varepsilon) := (x - m^\varepsilon_{\rm jkl})/\varepsilon$ and make the ansatz

$$\boldsymbol{u}_{\rm tp}(x) = \sum_{k=0}^{\infty} \varepsilon^k \boldsymbol{\mathcal{U}}_k(y(x,\varepsilon)), \quad \boldsymbol{p}_{\rm tp}(x) = \sum_{k=0}^{\infty} \varepsilon^k \boldsymbol{\mathcal{P}}_k(y(x,\varepsilon)),$$

and

$$\boldsymbol{\varphi}_{\rm tp}(x) = \sum_{k=0}^{\infty} \varepsilon^k \boldsymbol{\Theta}_k(y(x,\varepsilon)),$$

where $\boldsymbol{\Theta}_0(y(x,\varepsilon)) \in \Sigma^N$ and $\boldsymbol{\Theta}_k(y(x,\varepsilon)) \in T\Sigma^N$ $\forall k \geq 1$. We substitute this into the first order optimality system in Theorem 4.6 and then expand y in powers of ε.

The $\mathcal{O}(\frac{1}{\varepsilon^2})$-system reads

$$\begin{cases} -\nabla_y \cdot \left[\overline{\mathbb{C}}(\boldsymbol{\Theta}_0)\mathcal{E}(\boldsymbol{\mathcal{U}}_0)\right] = \boldsymbol{0} \ (\mathrm{SE})^{\rm tp}, \\ -\nabla_y \cdot \left[\overline{\mathbb{C}}(\boldsymbol{\Theta}_0)\mathcal{E}(\boldsymbol{\mathcal{P}}_0)\right] = \boldsymbol{0} \ (\mathrm{AE})^{\rm tp}, \\ -\boldsymbol{P}_{T\Sigma}(\overline{\mathbb{C}}'(\boldsymbol{\Theta}_0)\mathcal{E}(\boldsymbol{\mathcal{P}}_0)\mathcal{E}(\boldsymbol{\mathcal{U}}_0)) = \boldsymbol{0} \ (\mathrm{GE})^{\rm tp}. \end{cases}$$

The adjoint and the state equation allow for solutions constant in z and since matching implies that $\boldsymbol{\mathcal{P}}_0$ and $\boldsymbol{\mathcal{U}}_0$ remain bounded these are the only solutions. Here one can use arguments as in [36], see Theorem 4.16 (Liouville theorem). For these constant solutions the gradient equation is also fulfilled. Using the fact that $\boldsymbol{\mathcal{P}}_0$ and $\boldsymbol{\mathcal{U}}_0$ are constant and (5.17) the $\mathcal{O}(\frac{1}{\varepsilon})$-system reads

$$-\Delta_y \boldsymbol{\Theta}_0 + \boldsymbol{P}_{T\Sigma}\Psi_0'(\boldsymbol{\Theta}_0) = 0.$$

We are looking for a solution of this equation that connects $\boldsymbol{e}_j$ to $\boldsymbol{e}_k$ at $+\infty$ across $\Gamma^\varepsilon_{\rm jk}$, $\boldsymbol{e}_k$ to $\boldsymbol{e}_l$ at $+\infty$ across $\Gamma^\varepsilon_{\rm kl}$ and $\boldsymbol{e}_l$ to $\boldsymbol{e}_j$ at $+\infty$ across $\Gamma^\varepsilon_{\rm lj}$ in form of the associated one-dimensional stationary wave solutions, see [14,15,46] for details. Such a solution exists only if the force balance condition

$$\sigma_{\rm jk}\nu^0_{\rm jk} + \sigma_{\rm kl}\nu^0_{\rm kl} + \sigma_{\rm lj}\nu^0_{\rm lj} = 0$$

https://doi.org/10.1051/cocv/2014006 Published online by Cambridge University Press

is satisfied. This identity admits a solution if and only if the coefficients $\sigma_{\rm ab}$ fulfill $\sigma_{\rm ab}+\sigma_{\rm bc}\geq\sigma_{\rm ca}$ for any cyclic permutation (a,b,c) of (j,k,l). But, since in the present case, $\sigma_{\rm ab}$ can be characterized as

$$d(\boldsymbol{e}_a,\boldsymbol{e}_b):=\inf\left\{\int_0^1 \Psi_0^{\frac{1}{2}}(\varrho(t))|\varrho'(t)|\mathrm{d}t\mid \varrho\in C^1([0,1],\mathbb{R}^d),\varrho(0)=\boldsymbol{e}_a,\varrho(1)=\boldsymbol{e}_b\right\},$$

see [4], here this constraint is always fulfilled which follows from the triangle inequality for d. The angles at the junction satisfy Young's law which is given as

$$\frac{\sin\theta_{\rm jk}}{\sigma_{\rm jk}}=\frac{\sin\theta_{\rm kl}}{\sigma_{\rm kl}}=\frac{\sin\theta_{\rm lj}}{\sigma_{\rm lj}},$$

where $\theta_{\rm ab}$ is the angle between the vectors $\nu^0_{\rm bc}$ and $\nu^0_{\rm ca}$.

Remark 5.1. In applications to multi-structural topology optimization it is desirable that at a triple junction involving void the angle of the void is close to π. If this would not be the case one would expect high stresses at the junction which could lead to damage. Certain given angles can be achieved in the sharp interface limit of the phase field model by choosing the function Ψ_0 appropriately, see [31].

5.4. The limit problem and its geometric properties

As mentioned before the domain Ω is partitioned into N regions Ω^i, $i\in\{1,\dots,N\}$, which are separated by interfaces $\Gamma_{\rm ij}$, $i<j$. We remark that for $\delta>0$ small we have $x+\delta\boldsymbol{\nu}\in\Omega^j$ and $x-\delta\boldsymbol{\nu}\in\Omega^i$. Moreover we define $[\boldsymbol{w}]_i^j:=\lim\limits_{\delta\searrow 0}(\boldsymbol{w}(x+\delta\boldsymbol{\nu})-\boldsymbol{w}(x-\delta\boldsymbol{\nu}))$. We obtain for $i,j\in\{1,\dots,N-1\}$:

$$(\mathrm{SE})^i\begin{cases}-\nabla\cdot\left[\mathbb{C}^i\mathcal{E}(\boldsymbol{u})\right]=\boldsymbol{f} & \text{in } \Omega^i,\\ [\boldsymbol{u}]_i^j=\boldsymbol{0} & \text{on } \Gamma_{\rm ij},\\ [\mathbb{C}\mathcal{E}(\boldsymbol{u})\boldsymbol{\nu}]_i^j=\boldsymbol{0} & \text{on } \Gamma_{\rm ij},\\ \boldsymbol{u}=\boldsymbol{0} & \text{on } \Gamma_D\cap\partial\Omega^i,\\ \left[\mathbb{C}^i\mathcal{E}(\boldsymbol{u})\right]\boldsymbol{n}=\boldsymbol{g} & \text{on } \Gamma_g\cap\partial\Omega^i,\\ \left[\mathbb{C}^i\mathcal{E}(\boldsymbol{u})\right]\boldsymbol{n}=\boldsymbol{0} & \text{on } \Gamma_0\cap\partial\Omega^i,\end{cases}$$

$$(\mathrm{AE})^i\begin{cases}-\nabla\cdot\left[\mathbb{C}^i\mathcal{E}(\boldsymbol{p})\right]=\alpha\boldsymbol{f}+2\beta\nu J_0(\boldsymbol{u},\boldsymbol{\varphi})^{\frac{\nu-1}{\nu}}c(\boldsymbol{u}-\boldsymbol{u}_\Omega) & \text{in } \Omega^i,\\ [\boldsymbol{p}]_i^j=\boldsymbol{0} & \text{on } \Gamma_{\rm ij},\\ [\mathbb{C}\mathcal{E}(\boldsymbol{p})\boldsymbol{\nu}]_i^j=\boldsymbol{0} & \text{on } \Gamma_{\rm ij},\\ \boldsymbol{p}=\boldsymbol{0} & \text{on } \Gamma_D\cap\partial\Omega^i,\\ \left[\mathbb{C}^i\mathcal{E}(\boldsymbol{p})\right]\boldsymbol{n}=\alpha\boldsymbol{g} & \text{on } \Gamma_g\cap\partial\Omega^i,\\ \left[\mathbb{C}^i\mathcal{E}(\boldsymbol{p})\right]\boldsymbol{n}=\boldsymbol{0} & \text{on } \Gamma_0\cap\partial\Omega^i,\end{cases}$$

and we have $\mathbb{C}^i\mathcal{E}_i(\boldsymbol{u})\boldsymbol{\nu}=\mathbb{C}^i\mathcal{E}_i(\boldsymbol{p})\boldsymbol{\nu}=\boldsymbol{0}$ on $\Gamma_{\rm iN}$. Moreover we obtain for all $i,j\neq N$

$$0=\gamma\sigma_{\rm ij}\kappa-[\mathbb{C}\mathcal{E}(\boldsymbol{u}):\mathcal{E}(\boldsymbol{p})]_i^j+[\mathbb{C}\mathcal{E}(\boldsymbol{u})\boldsymbol{\nu}\cdot(\nabla\boldsymbol{p})\boldsymbol{\nu}]_i^j+[\mathbb{C}\mathcal{E}(\boldsymbol{p})\boldsymbol{\nu}\cdot(\nabla\boldsymbol{u})\boldsymbol{\nu}]_i^j-\lambda^j+\lambda^i\ \text{ on } \Gamma_{\rm ij}\tag{5.22}$$

and remark that the terms involving $\boldsymbol{u}$ and $\boldsymbol{p}$ generalize the Eshelby traction known from materials science, see [28,29]. In addition for all $i\neq N$ it holds

$$0=\gamma\sigma_{\rm iN}\kappa+\mathbb{C}^i\mathcal{E}_i(\boldsymbol{u}):\mathcal{E}_i(\boldsymbol{p})-\beta\nu J_0(\boldsymbol{u},\boldsymbol{\varphi})^{\frac{\nu-1}{\nu}}c\,|\boldsymbol{u}-\boldsymbol{u}_\Omega|^2-\boldsymbol{f}\cdot(\alpha\boldsymbol{u}+\boldsymbol{p})+\lambda^i-\lambda^N\ \text{ on } \Gamma_{\rm iN}.$$

https://doi.org/10.1051/cocv/2014006 Published online by Cambridge University Press

Remark 5.2. In the case of $N = 2$ we have $\Omega = \Omega^M \cup \Omega^V$, where Ω^M and Ω^V denote the material and the void part of the domain. The interface which separates the two phases is denoted by Γ_{MV}. Using the notation $\Gamma_k^M := \Gamma_k \cap \partial\Omega^M$, $k \in \{D, g, 0\}$ we obtain as the limit problem

$$(\mathrm{SE})^{MV} \begin{cases} -\nabla \cdot \left[\mathbb{C}^M \mathcal{E}(\boldsymbol{u})\right] = \boldsymbol{f} & \text{in } \Omega^M, \\ \left[\mathbb{C}^M \mathcal{E}_M(\boldsymbol{u})\right] \boldsymbol{\nu} = \boldsymbol{0} & \text{on } \Gamma_{MV}, \\ \boldsymbol{u} = \boldsymbol{0} & \text{on } \Gamma_D^M, \\ \left[\mathbb{C}^M \mathcal{E}(\boldsymbol{u})\right] \boldsymbol{n} = \boldsymbol{g} & \text{on } \Gamma_g^M, \\ \left[\mathbb{C}^M \mathcal{E}(\boldsymbol{u})\right] \boldsymbol{n} = \boldsymbol{0} & \text{on } \Gamma_0^M, \end{cases}$$

$$(\mathrm{AE})^{MV} \begin{cases} -\nabla \cdot \left[\mathbb{C}^M \mathcal{E}(\boldsymbol{p})\right] = \alpha \boldsymbol{f} + 2\beta\nu J_0(\boldsymbol{u}, \boldsymbol{\varphi})^{\frac{\nu-1}{\nu}} c(\boldsymbol{u} - \boldsymbol{u}_\Omega) & \text{in } \Omega^M, \\ \left[\mathbb{C}^M \mathcal{E}_M(\boldsymbol{p})\right] \boldsymbol{\nu} = \boldsymbol{0} & \text{on } \Gamma_{MV}, \\ \boldsymbol{p} = \boldsymbol{0} & \text{on } \Gamma_D^M, \\ \left[\mathbb{C}^M \mathcal{E}(\boldsymbol{p})\right] \boldsymbol{n} = \alpha \boldsymbol{g} & \text{on } \Gamma_g^M, \\ \left[\mathbb{C}^M \mathcal{E}(\boldsymbol{p})\right] \boldsymbol{n} = \boldsymbol{0} & \text{on } \Gamma_0^M, \end{cases}$$

and we have the equation:

$$0 = \gamma\sigma_{MV}\kappa + \mathbb{C}^M \mathcal{E}_M(\boldsymbol{u}) : \mathcal{E}_M(\boldsymbol{p}) - \beta\nu J_0(\boldsymbol{u}, \boldsymbol{\varphi})^{\frac{\nu-1}{\nu}} c\,|\boldsymbol{u} - \boldsymbol{u}_\Omega|^2 - \boldsymbol{f} \cdot (\alpha\boldsymbol{u} + \boldsymbol{p}) + \lambda^{MV} \quad \text{on } \Gamma_{MV}, \tag{5.23}$$

where λ^{MV} is the difference of the Lagrange multipliers λ^M and λ^V discussed further above.

5.5. Relating the sharp interface limit to classical shape calculus

In this subsection we compare the limit problem in Section 5.4 and especially (5.23) with results of [3], which were obtained using classical shape calculus. For this purpose we reformulate the results in [3] to our setting. Let $\Omega \subset \mathbb{R}^d$ be defined as in Remark 5.2, that means $\Omega = \Omega^M \cup \Omega^V$. Given $(\boldsymbol{f}, \boldsymbol{g}, \boldsymbol{u}_\Omega, c) \in L^2(\Omega, \mathbb{R}^d) \times L^2(\Gamma_g, \mathbb{R}^d) \times L^2(\Omega, \mathbb{R}^d) \times L^\infty(\Omega)$, measurable sets $S_i \subseteq \Omega$, $i \in \{0, 1\}$, with $S_0 \cap S_1 = \emptyset$, objective functions

$$F(\Omega^M) = \int_{\Omega^M} \boldsymbol{f} \cdot \boldsymbol{u} + \int_{\Gamma_g^M} \boldsymbol{g} \cdot \boldsymbol{u}, \tag{5.24}$$

$$J_0(\Omega^M) := \left(\int_{\Omega^M} c\,|\boldsymbol{u} - \boldsymbol{u}_\Omega|^2 \right)^\nu, \quad \nu \in (0, 1] \tag{5.25}$$

and the perimeter $P(\Omega^M) = \int\limits_{(\partial\Omega^M)\cap\Omega} \mathrm{d}s$ of Ω^M in Ω the optimization problem is

$$(\mathcal{P}^0) \qquad \begin{cases} \min & J(\Omega^M) := \alpha F(\Omega^M) + \beta J_0(\Omega^M) + \gamma\sigma_{MV} P(\Omega^M), \\ \text{over} & \mathcal{U}_d = \{\Omega^M \subset \Omega \text{ such that } |\Omega^M| = V \text{ and } S_0 \subset \Omega^M,\ S_1 \subset \Omega^V\}, \\ \text{s.t.} & (\mathrm{SE})^{MV} \begin{cases} -\nabla \cdot \left[\mathbb{C}^M \mathcal{E}(\boldsymbol{u})\right] = \boldsymbol{f} & \text{in } \Omega^M, \\ \left[\mathbb{C}^M \mathcal{E}_M(\boldsymbol{u})\right] \boldsymbol{\nu} = \boldsymbol{0} & \text{on } \Gamma_{MV}, \\ \boldsymbol{u} = \boldsymbol{0} & \text{on } \Gamma_D^M, \\ \left[\mathbb{C}^M \mathcal{E}(\boldsymbol{u})\right] \boldsymbol{n} = \boldsymbol{g} & \text{on } \Gamma_g^M, \\ \left[\mathbb{C}^M \mathcal{E}(\boldsymbol{u})\right] \boldsymbol{n} = \boldsymbol{0} & \text{on } \Gamma_0^M. \end{cases} \end{cases}$$

https://doi.org/10.1051/cocv/2014006 Published online by Cambridge University Press

Note that $\partial\Omega^M = \Gamma_D^M \cup \Gamma_g \cup \Gamma_0^M \cup \Gamma_{MV}$. The authors in [3] used shape calculus and formulated the following theorem:

Theorem 5.3. *Let Ω^M be a smooth bounded open set and $\boldsymbol{\theta} \in W^{1,\infty}(\mathbb{R}^d;\mathbb{R}^d)$, with $\boldsymbol{\theta}\cdot\boldsymbol{n} = 0$ on $\partial\Omega^M \setminus \Gamma_{MV}$. Furthermore let κ be the mean curvature of Γ_{MV}. Assume that $\boldsymbol{f}$ and the solution $\boldsymbol{u}$ of the state equation are smooth, say $\boldsymbol{f} \in H^1(\Omega^M,\mathbb{R}^d)$ and $\boldsymbol{u} \in H^2(\Omega^M,\mathbb{R}^d)$. In addition we assume that $\boldsymbol{g}$ is defined on $\partial\Omega$. The shape derivative of $J(\Omega^M)$ at Ω^M in the direction $\boldsymbol{\theta}$ is given by*

$$\begin{aligned} J'(\Omega^M)(\boldsymbol{\theta}) = &- \int_{\Gamma_{MV}} \left(\gamma\sigma_{MV}\kappa + \mathbb{C}^M\mathcal{E}(\boldsymbol{u}) : \mathcal{E}(\boldsymbol{p})\right)\boldsymbol{\theta}\cdot\boldsymbol{n}\,\mathrm{d}s \\ &+ \int_{\Gamma_{MV}} \left(\beta\nu J_0(\boldsymbol{u},\boldsymbol{\varphi})^{\frac{\nu-1}{\nu}} c|\boldsymbol{u}+\boldsymbol{u}_\Omega|^2\right)\boldsymbol{\theta}\cdot\boldsymbol{n}\,\mathrm{d}s \\ &+ \int_{\Gamma_{MV}} (\boldsymbol{f}\cdot(\alpha\boldsymbol{u}+\boldsymbol{p}))\,\boldsymbol{\theta}\cdot\boldsymbol{n}\,\mathrm{d}s, \end{aligned} \tag{5.26}$$

where $\boldsymbol{p}$ is the adjoint state, assumed to be smooth, i.e. $\boldsymbol{p} \in H^2(\Omega,\mathbb{R}^d)$, defined as the solution of

$$(AE)^{MV} \begin{cases} -\nabla\cdot\left[\mathbb{C}^M\mathcal{E}(\boldsymbol{p})\right] = \alpha\boldsymbol{f} + 2\beta\nu J_0(\boldsymbol{u},\boldsymbol{\varphi})^{\frac{\nu-1}{\nu}} c(\boldsymbol{u}-\boldsymbol{u}_\Omega) & \text{in } \Omega^M, \\ \left[\mathbb{C}^M\mathcal{E}_M(\boldsymbol{p})\right]\boldsymbol{\nu} = \boldsymbol{0} & \text{on } \Gamma_{MV}, \\ \boldsymbol{p} = \boldsymbol{0} & \text{on } \Gamma_D^M, \\ \left[\mathbb{C}^M\mathcal{E}(\boldsymbol{p})\right]\boldsymbol{n} = \alpha\boldsymbol{g} & \text{on } \Gamma_g^M, \\ \left[\mathbb{C}^M\mathcal{E}(\boldsymbol{p})\right]\boldsymbol{n} = \boldsymbol{0} & \text{on } \Gamma_0^M. \end{cases}$$

In contrast to [3] we define $\boldsymbol{g}$ on $\partial\Omega$ and in addition we use a different sign convention for the mean curvature κ and the adjoint state $\boldsymbol{p}$. We notice that the shape calculus approach, see (5.26), coincides with the results we get by the asymptotic expansion of the phase field optimality system, see (5.23). This follows since at a minimum of $(\mathcal{P}^0)$ we have to take volume constraints into account. Hence (5.26) leads to (5.23) with a Lagrange multiplier λ^{MV} which is related to the volume constraint.

6. Numerical simulations

In this section we derive a finite element approximation of the phase field topology optimization problem and discuss some computational results.

In order to solve the gradient inequality in Theorem 4.6, we use a gradient flow dynamic, see [8–10], for the reduced functional yielding the following variational inequality for all $\tilde{\boldsymbol{\varphi}} \in \boldsymbol{\mathcal{G}^m} \cap \boldsymbol{U_c}$ and all $t > 0$:

$$\begin{aligned} &\varepsilon\int_\Omega \frac{\partial\boldsymbol{\varphi}}{\partial t}(\tilde{\boldsymbol{\varphi}}-\boldsymbol{\varphi}) + \gamma\varepsilon\int_\Omega \nabla\boldsymbol{\varphi} : \nabla(\tilde{\boldsymbol{\varphi}}-\boldsymbol{\varphi}) + \frac{\gamma}{\varepsilon}\int_\Omega \Psi_0'(\boldsymbol{\varphi})\cdot(\tilde{\boldsymbol{\varphi}}-\boldsymbol{\varphi}) \\ &-\beta\nu J_0(\boldsymbol{u},\boldsymbol{\varphi})^{\frac{\nu-1}{\nu}}\int_\Omega c(\tilde{\varphi}^N-\varphi^N)|\boldsymbol{u}-\boldsymbol{u}_\Omega|^2 \\ &-\int_\Omega(\tilde{\varphi}^N-\varphi^N)\boldsymbol{f}\cdot(\alpha\boldsymbol{u}+\boldsymbol{p}) - \langle\mathcal{E}(\boldsymbol{p}),\mathcal{E}(\boldsymbol{u})\rangle_{\mathbb{C}'(\boldsymbol{\varphi})(\tilde{\boldsymbol{\varphi}}-\boldsymbol{\varphi})} \geq 0. \end{aligned} \tag{6.1}$$

This is a (vector-valued) Allen–Cahn inequality with a forcing term related to elastic effects, see also [8–10]. If $\frac{\partial\boldsymbol{\varphi}(\tilde{t},\cdot)}{\partial t} = \boldsymbol{0}$ in (6.1) then $\boldsymbol{\varphi}(\tilde{t},\cdot)$ is a solution of (GI) in Theorem 4.6. In the numerical experiments we always choose $\boldsymbol{f} \equiv \boldsymbol{0}$ which means no forces act in the interior.

For discretization in space we use the following finite element approximation, see also for example [8]. Here we assume for simplicity that Ω is a polyhedral domain and we let $\mathcal{T}_h$ be a regular triangulation of Ω into

https://doi.org/10.1051/cocv/2014006 Published online by Cambridge University Press

disjoint open simplices T. We define $h := \max_{T\in\mathcal{T}_h}\{\text{diam } T\}$ the maximal element size of $\mathcal{T}_h$. Associated with $\mathcal{T}_h$ is the piecewise linear finite element space

$$S^h := \left\{\phi \in C^0(\overline{\Omega}) \,\middle|\, \phi\big|_T \in P_1(T) \ \forall\, T \in \mathcal{T}_h\right\} \subset H^1(\Omega),$$

where we denote by $P_1(T)$ the set of all affine functions on T. Furthermore we define

$$\boldsymbol{S}_D^h(\Omega,\mathbb{R}^d) = \left\{\boldsymbol{v} \in (S^h)^d \,\middle|\, \boldsymbol{v} = \boldsymbol{0} \text{ on } \Gamma_D\right\} \subset H_D^1(\Omega,\mathbb{R}^d),$$

$$\boldsymbol{\mathcal{G}}_{\boldsymbol{h}}^{\boldsymbol{m}} := \{\boldsymbol{\chi} \in (S^h)^N |\ \boldsymbol{\chi} \geq \boldsymbol{0},\ \fint_\Omega \boldsymbol{\chi} = \boldsymbol{m} \text{ and } \sum_{i=1}^N \chi_i = 1 \quad \text{in } \Omega\}$$

and

$$\boldsymbol{U}_c^h := \{\boldsymbol{\chi} \in (S^h)^N |\ (\chi^N)\big|_T \equiv 0 \text{ for } T \subseteq S_0,\ \left(\chi^N\right)\big|_T \equiv 1 \text{ for } T \subseteq S_1,\ T \in \mathcal{T}_h\}.$$

In time we apply a semi-implicit discretization with a fixed time step τ. The resulting method can also be interpreted as a pseudo-time stepping approach to (GI). We obtain the following iterative procedure:
Set $n = 0$ and start with an initial guess $\boldsymbol{\varphi}_h^0 \in \boldsymbol{\mathcal{G}}_{\boldsymbol{h}}^{\boldsymbol{m}} \cap \boldsymbol{U}_c^h$. Then solve successively with respect to n the following inequality for the solution $\boldsymbol{\varphi}_h^{n+1} \in \boldsymbol{\mathcal{G}}_{\boldsymbol{h}}^{\boldsymbol{m}} \cap \boldsymbol{U}_c^h$ in the $(n+1)$th (artifical) time step

$$\begin{aligned}
&\frac{\varepsilon}{\tau}\int_\Omega (\boldsymbol{\varphi}_h^{n+1} - \boldsymbol{\varphi}_h^n)(\tilde{\boldsymbol{\varphi}}_h - \boldsymbol{\varphi}_h^{n+1}) + \gamma\varepsilon \int_\Omega \nabla\boldsymbol{\varphi}_h^{n+1} : \nabla(\tilde{\boldsymbol{\varphi}}_h - \boldsymbol{\varphi}_h^{n+1}) \\
&\quad + \frac{\gamma}{\varepsilon}\int_\Omega \Psi_0'(\boldsymbol{\varphi}_h^n)\cdot(\tilde{\boldsymbol{\varphi}}_h - \boldsymbol{\varphi}_h^{n+1}) \\
&\quad - \beta\nu J_0(\boldsymbol{u}_h^n, \boldsymbol{\varphi}_h^n)^{\frac{\nu-1}{\nu}} \int_\Omega c(\tilde{\varphi}_h^N - \varphi_h^{N,n+1})|\boldsymbol{u}_h^n - \boldsymbol{u}_\Omega|^2 \\
&\quad - \langle \mathcal{E}(\mathbf{p}_h^n), \mathcal{E}(\boldsymbol{u}_h^n)\rangle_{\mathbb{C}'(\boldsymbol{\varphi}_h^n)(\tilde{\boldsymbol{\varphi}}_h - \boldsymbol{\varphi}_h^n)} \geq 0 \quad \forall \tilde{\boldsymbol{\varphi}}_h \in \boldsymbol{\mathcal{G}}_{\boldsymbol{h}}^{\boldsymbol{m}} \cap \boldsymbol{U}_c^h
\end{aligned} \tag{6.2}$$

where $\boldsymbol{p}_h^n, \boldsymbol{u}_h^n \in \boldsymbol{S}_D^h(\Omega,\mathbb{R}^d)$ are solutions of the following finite element approximations of the adjoint equation and the state equation

$$\langle \mathcal{E}(\boldsymbol{p}_h^n), \mathcal{E}(\boldsymbol{q}_h)\rangle_{\mathbb{C}(\boldsymbol{\varphi}_h^n)} = \int_\Omega 2\beta\nu J_0(\boldsymbol{u}_h^n, \boldsymbol{\varphi}_h^n)^{\frac{\nu-1}{\nu}} c(1-\varphi_h^{N,n})(\boldsymbol{u}_h^n - \boldsymbol{u}_\Omega)\cdot\boldsymbol{q}_h + \alpha\int_{\Gamma_g} \boldsymbol{g}\cdot\boldsymbol{q}_h \quad \forall \boldsymbol{q}_h \in \boldsymbol{S}_D^h, \tag{6.3}$$

$$\langle \mathcal{E}(\boldsymbol{u}_h^n), \mathcal{E}(\boldsymbol{v}_h)\rangle_{\mathbb{C}(\boldsymbol{\varphi}_h^n)} = \int_{\Gamma_g} \boldsymbol{g}\cdot\boldsymbol{v}_h \quad \forall \boldsymbol{v}_h \in \mathbf{S}_D^h. \tag{6.4}$$

We use a preconditioned conjugate gradient solver for (6.3) and (6.4), see also [34]. To solve (6.2) we use the primal-dual active set method presented in [8]. To the resulting system of linear equations we apply the direct solver UMFPACK [22] when $d = 2$ and MINRES when $d = 3$.

We note that the thickness of the interfacial layer between bulk regions is proportional to ε. In order to resolve this interfacial layer we need to choose $h \ll \varepsilon$, see [23] for details. Away from the interface h can be chosen larger and hence adaptivity in space can heavily speed up computations. In fact we use the finite element toolbox Alberta 2.0, see [51] for adaptivity and we implemented the same mesh refinement strategy as in [6], *i.e.* a fine mesh is constructed for all variables $\boldsymbol{\varphi}_h^{n+1}, \boldsymbol{p}_h^n$ and $\boldsymbol{u}_h^n$ where $0 < (\varphi_h^n)^i < 1$ for at least one index $i \in \{1,\dots,N\}$ and with a coarser mesh present in the bulk regions where $(\varphi_h^n)^i = 0$ or $(\varphi_h^n)^i = 1$ for all $i \in \{1,\dots,N\}$.

Unless otherwise stated in the two dimensional simulations we choose as the minimal diameter of all elements $h_{\min} = \frac{1}{128}$, the maximal diameter $h_{\max} = \frac{1}{16}$ and the time-step $\tau = 1.0\cdot 10^{-6}$. In the three dimensional simulation we take $h_{\min} = \frac{1}{90}$, $h_{\max} = \frac{1}{16}$ and $\tau = 1.0\times 10^{-5}$. When there is only one material present, *i.e.*

https://doi.org/10.1051/cocv/2014006 Published online by Cambridge University Press

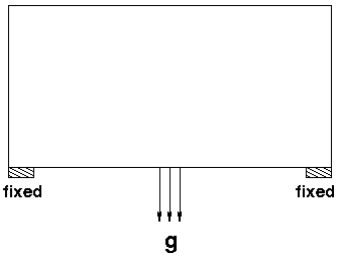


FIGURE 2. Bridge configuration.

$N = 2$, then void is described by $\varphi^2 = 1 - \varphi^1$. Thus the vector-valued Allen−Cahn inequality with two order parameters is reduced in the computations to a scalar Allen−Cahn inequality. In all cases the iteration stops when $\boldsymbol{\varphi}$ does visually not change anymore.

In Sections 6.1−6.3 we display numerical results with $\beta = 0$ (in this case it holds $\boldsymbol{p}_h^n = \alpha \boldsymbol{u}_h^n$). This minimum compliance problem aims to construct a structure with maximal global stiffness and is a basic problem in topology optimization, see [7]. Other numerical approaches based on a phase field method can be found *e.g.* in [9, 50, 55, 60, 61]. Unless otherwise stated in our examples we set the matrix $\mathcal{W}$ in the bulk potential term to be $\mathbf{1} \otimes \mathbf{1} - \mathrm{Id}$ and the interfacial parameters are taken to be $\gamma = 1$ with $\varepsilon = \frac{1}{16\pi}$ for $d = 2$ and $\varepsilon = \frac{1}{8\pi}$ for $d = 3$. Moreover, we set $S_0 = S_1 = \emptyset$ and hence $\boldsymbol{U}_c = H^1(\Omega, \mathbb{R}^N)$ and $\boldsymbol{\mathcal{G}}_{\boldsymbol{h}}^{\boldsymbol{m}} \cap \boldsymbol{U}_c^h = \boldsymbol{\mathcal{G}}_{\boldsymbol{h}}^{\boldsymbol{m}}$.

In Section 6.4 we present results with $\alpha = 0$. In this case we want to optimize the error compared to a target displacement (compliant mechanism). Also this is a standard problem in topology optimization and we refer to [3, 7, 55] for further details. For our simulation we choose an example in which we aim to minimize the total displacement under a force acting on the boundary, for the setup see Figure 9. Such a situation is typical in applications, see [7]. For numerical simulations for the compliant mechanism using the SIMP method we refer to [7] whereas in [3] the level set method is used and in [55] a phase field method is used to numerically solve the problem.

6.1. Bridge construction with $N = 2$ and $d = 2$

The classical problem of the bridge configuration – depicted in Figure 2 – is considered first. We pose Dirichlet boundary conditions on the bottom left and right boundaries Γ_D and a vertical force is acting on the bottom at the centre. We take $\Omega = (-1, 1) \times (0, 1)$ and $\Gamma_D = \{(x, 0) \in \mathbb{R}^2 : x \in (-1, -0.9] \cup [0.9, 1)\}$. The force F is acting on $\Gamma_g := \{(x, 0) \in \mathbb{R}^2 : x \in [-0.02, 0.02]\}$ and is defined by a constant function $\boldsymbol{g} \equiv (0, -5000)^T$ on Γ_g. In our computations we use an isotropic elasticity tensor $\mathbb{C}_1$ of the form $\mathbb{C}_1\mathcal{E} = 2\mu_1\mathcal{E} + \lambda_1(tr\mathcal{E})I$ with the Lamé constants $\lambda_1 = \mu_1 = 250$ and choose $\mathbb{C}_2 = \varepsilon^2\mathbb{C}_1$ in the void. Moreover, we assume as much void as material, hence $\boldsymbol{m} = (\frac{1}{2}, \frac{1}{2})^T$. We display results from two sets of initial data, the first in which we set $\boldsymbol{\varphi}_h^0 \equiv (\frac{1}{2}, \frac{1}{2})^T$ and the second in which we take a checkerboard structure alternating regions with $\boldsymbol{\varphi}_h^0 \equiv (0, 1)^T$ and $\boldsymbol{\varphi}_h^0 \equiv (1, 0)^T$, both sets of data ensure that we approximately have the same proportion of material and void.

In Figures 3 and 4 we see that although the two sets of initial data give rise to different evolutions the final solution is the same. We point out that the connectivity of the regions occupied by material is found by the method without using informations on topological derivatives. One also observes several topological changes during time, see also [60, 61].

6.2. Cantilever beam construction with $N = 3$ and $d = 2$

In this section we present a numerical simulation for a cantilever beam geometry, see Figure 5, consisting of hard as well as soft material and void. We pose Dirichlet boundary conditions on the left boundary Γ_D and a vertical force is acting at the bottom of its free vertical edge. We take $\Omega = (-1, 1) \times (0, 1)$, and hence $\Gamma_D = \{(-1, y) \in \mathbb{R}^2 : y \in (0, 1)\}$. The force F is acting on $\Gamma_g := \{(x, 0) \in \mathbb{R}^2 : x \in [0.75, 1)\}$ and is defined

https://doi.org/10.1051/cocv/2014006 Published online by Cambridge University Press

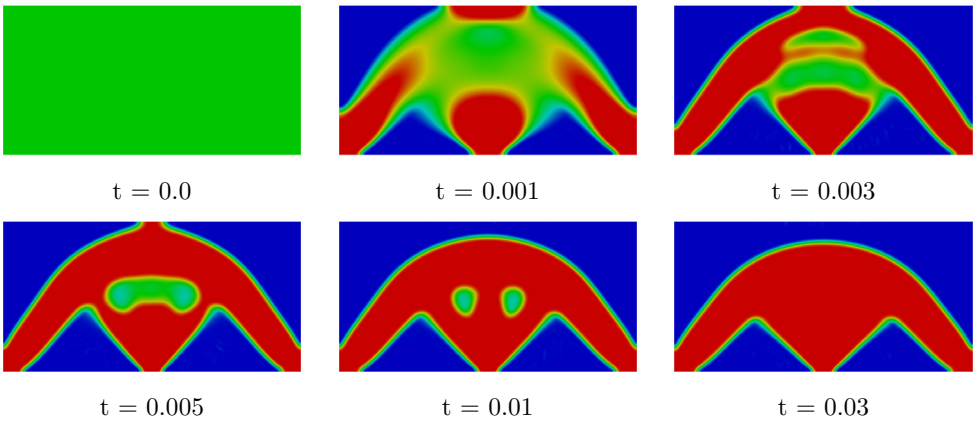


FIGURE 3. Bridge simulation with $N = 2$ and $\boldsymbol{\varphi}_h^0 \equiv (\frac{1}{2}, \frac{1}{2})^T$, material in red and void in blue.

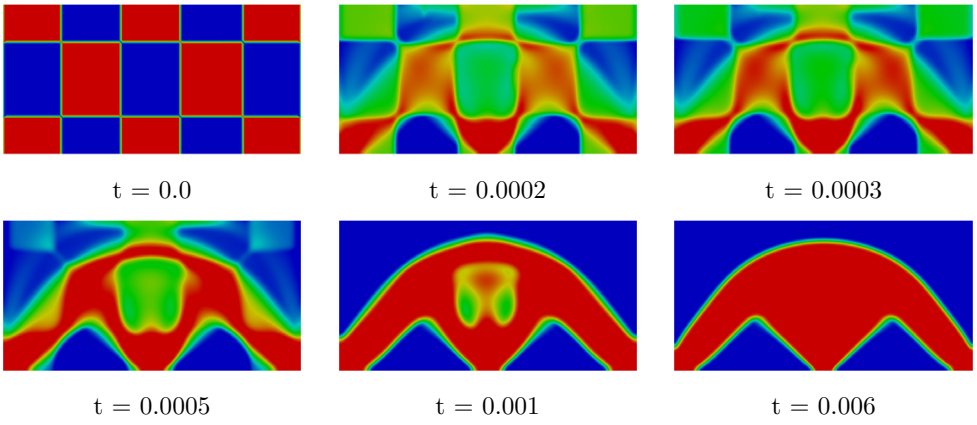


FIGURE 4. Bridge simulation with $N = 2$ and checkerboard initial data, material in red and void in blue.



FIGURE 5. Cantilever beam configuration.

https://doi.org/10.1051/cocv/2014006 Published online by Cambridge University Press

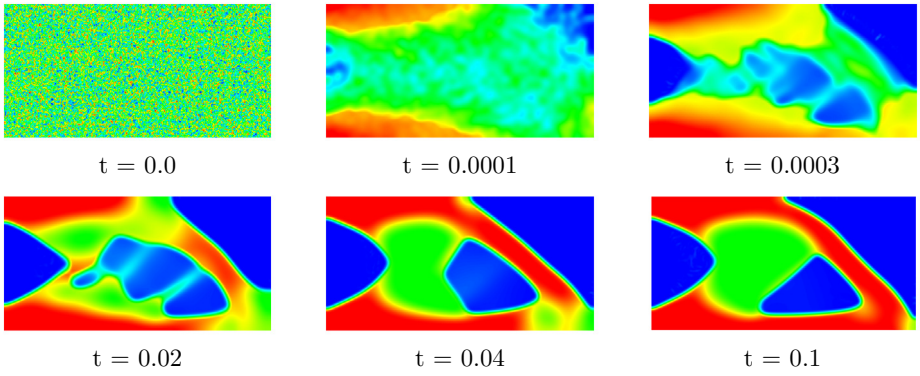


FIGURE 6. Cantilever beam simulation with $N = 3$ and $\mathcal{W}$ given by (6.5). Hard material in red, soft material in green and void in blue.

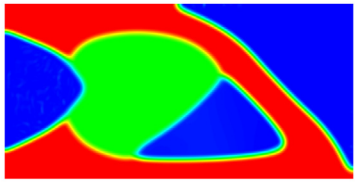


FIGURE 7. Cantilever beam simulation with $N = 3$ and $\mathcal{W} = \mathbf{1} \otimes \mathbf{1} - \mathrm{Id}$. Hard material in red, soft material in green and void in blue.

by $\boldsymbol{g} \equiv (0, -600)^T$ on Γ_g. We take $\gamma = 4$ and the mass constraints are set such that they enforce 36.5% hard material, 22% soft material and 41.5% void. For the hard material (associated with φ^1) we use the isotropic elasticity tensor $\mathbb{C}_1$ (see Sect. 6.1) and the Lamé constants $\lambda_1 = \mu_1 = 5000$; for the soft material (associated with φ^2) we choose $\mathbb{C}_2 = \frac{1}{2}\mathbb{C}_1$ and for the void we take $\mathbb{C}_3 = (2\varepsilon)^2\mathbb{C}_1$. A symmetric choice of Ψ would lead to 120° angles at the triple junction, see Section 5.3. When all these three phases meet at a triple point 120° it can be more likely that a crack forms. Hence, in structural topology optimization these 120° angle conditions at triple junctions are typically not wanted. To overcome this the matrix $\mathcal{W}$ in the bulk potential is adjusted. We take

$$\mathcal{W} = \begin{pmatrix} 0 & 0.1 & 1 \\ 0.1 & 0 & 1 \\ 1 & 1 & 0 \end{pmatrix} \tag{6.5}$$

which at a triple junction forces the angle in the void to be larger than the other two angles. This choice is motivated by the results in [31, 32].

We initialize the order parameter $\boldsymbol{\varphi}_h^0$ with random values such that the sum constraint is fulfilled and the proportions of hard material, soft material and void are as required. Figure 6 shows the results obtained, where $\boldsymbol{\varphi}$ at $t = 0.1$ appears to be a numerical steady state.

In Figure 7 we also display the final solution for the choice $\mathcal{W} = \mathbf{1} \otimes \mathbf{1} - \mathrm{Id}$ which leads to a potential that is symmetric in the $(\varphi^i)'$s, $i \in \{1, 2, 3\}$. We observe smaller angles in the void at the triple junction. Similar numerical results for such a symmetric situation have been obtained earlier in [60, 61].

https://doi.org/10.1051/cocv/2014006 Published online by Cambridge University Press

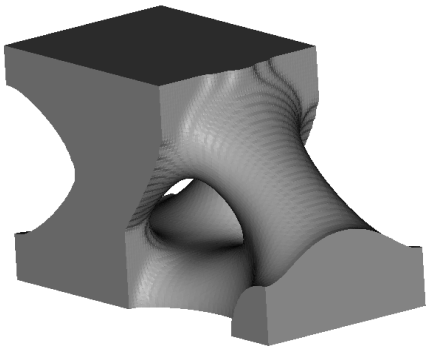


FIGURE 8. Cantilever beam simulation with $N = 2$, $d = 3$ and checkerboard initial data.

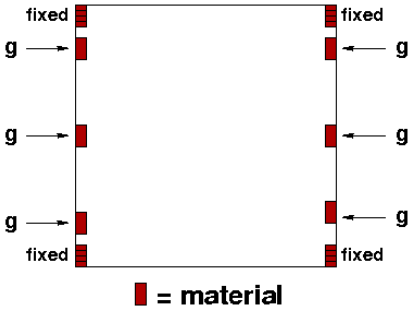


FIGURE 9. Push configuration.

6.3. Cantilever beam construction with $N = 2$ and $d = 3$

A numerical simulation for the extension of the cantilever beam geometry to three space dimensions is displayed in Figure 8. In particular we take $\boldsymbol{m} = (\frac{1}{2}, \frac{1}{2})^T$, $\Omega = (0,5) \times (0,2.5) \times (0,3)$, $\Gamma_D = \{(0,y,z) \in \mathbb{R}^3 : (y,z) \in (0,2.5) \times (0,3)\}$, $\Gamma_g := \{(x,y,0) \in \mathbb{R}^3 : (x,y) \in [4.75,5) \times (0,2.5)\}$ and $\boldsymbol{g} \equiv (0,0,-165)^T$ on Γ_g. We use an isotropic elasticity tensor $\mathbb{C}_1$ of the form $\mathbb{C}_1\mathcal{E} = 2\mu_1\mathcal{E} + \lambda_1(tr\mathcal{E})I$ with $\lambda_1 = \mu_1 = 5000$ and we choose $\mathbb{C}_2 = \varepsilon^2\mathbb{C}_1$ in the void. We initialize the order parameter $\boldsymbol{\varphi}$ with a similar checkerboard structure to that described in Section 6.1. In Figure 8 we display the boundary between the material and the void of the final solution.

6.4. Push construction with $N = 2$ and $d = 2$

For the construction problem under pushing forces we present numerical simulations for the configuration depicted in Figure 9 where one minimizes the target displacement only. We set therefore $\alpha = 0$ and choose $\beta = 10, \nu = 0.5$. We set $\gamma = 0.2$ and $h_{\min} = \frac{1}{94}$. We take the constant weighting factor $c \equiv 2000$ in $\Omega := (-1,1) \times (-1,1)$ and no displacement of the material as target, *i.e.* $\boldsymbol{u}_\Omega = \boldsymbol{0}$. Furthermore we pose Dirichlet boundary conditions on the top and bottom of both the left and right boundaries, in particular we set $\Gamma_D = \{(-1,y) \cup (1,y) \in \mathbb{R}^2 : y \in (-1,-0.9] \cup [0.9,1)\}$, and apply horizontal forces along the left and right boundaries, *i.e.* $\Gamma_{g_-} \cup \Gamma_{g_+}$ with $\Gamma_{g_\pm} := \{(\pm 1, y) \in \mathbb{R}^2 : y \in [-0.8,-0.7] \cup [-0.1,0.1] \cup [0.7,0.8]\}$ As forces we define $\boldsymbol{g} \equiv (\pm 7, 0)^T$ on $\Gamma_{g_\pm}$. As in Section 6.1 we use an isotropic elasticity tensor $\mathbb{C}_1$ of the form $\mathbb{C}_1\mathcal{E} = 2\mu_1\mathcal{E} + \lambda_1(tr\mathcal{E})I$ and $\mathbb{C}_2 = \varepsilon^2\mathbb{C}_1$ in the void with the Lamé constants $\lambda_1 = \mu_1 = 10$. However instead of using the linear interpolation, defined in (2.10), of $\boldsymbol{\varphi}$ in the elasticity tensor we use the following quadratic interpolation,

https://doi.org/10.1051/cocv/2014006 Published online by Cambridge University Press

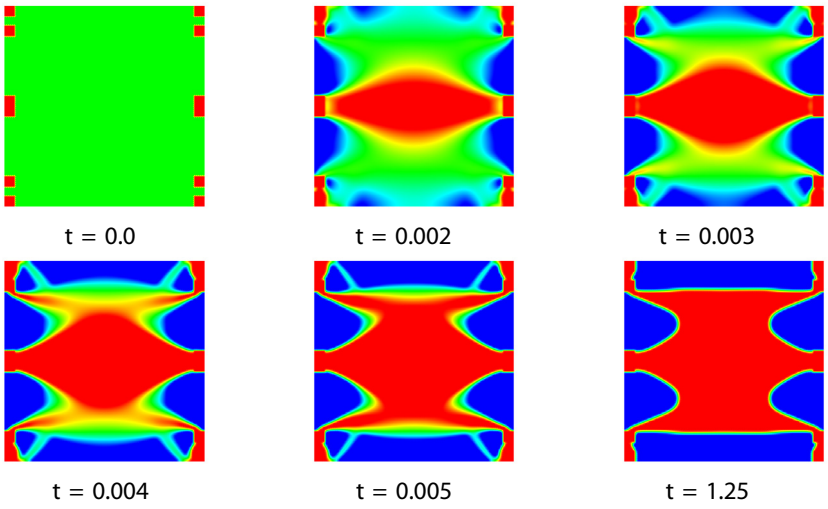


FIGURE 10. Push simulation with $N = 2$ and $\boldsymbol{\varphi}_h^0 = (\frac{1}{2}, \frac{1}{2})^T$ on $\Omega \setminus S_0$, material in red and void in blue.

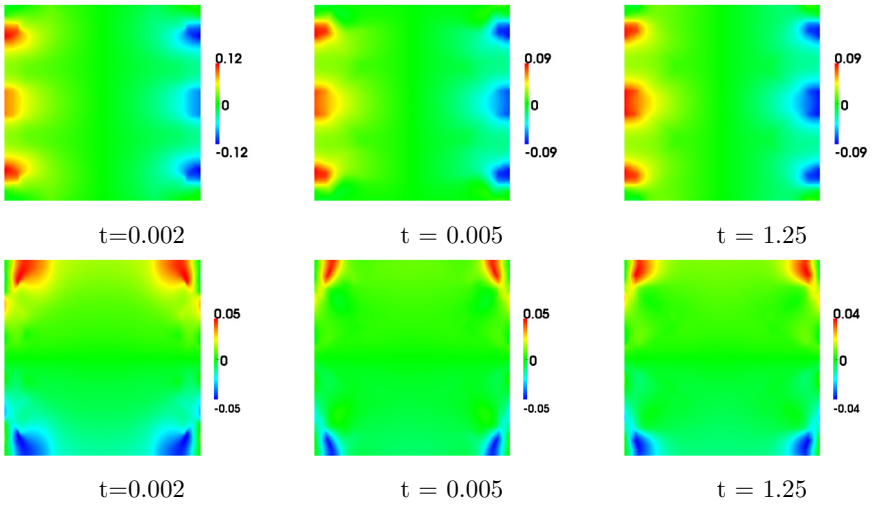


FIGURE 11. Displacement vector for the push simulation with $N = 2$ and $\boldsymbol{\varphi}_h^0 = (\frac{1}{2}, \frac{1}{2})^T$ on $\Omega \setminus S_0$; x-component top row, y component bottom row.

$\mathbb{C}(\boldsymbol{\varphi}) = (1-\varepsilon)^2(\varphi^1)^2\mathbb{C}^1 + \mathbb{C}^2$. Moreover, we enforce material in Ω, adjacent to the parts of the boundary that are fixed and where the forces are applied, by setting $S_0 = (-1,-0.9)\times(-1,-0.9) \cup (-1,-0.9)\times(0.9,1) \cup (0.9,1.0)\times(-1,-0.9) \cup (0.9,1)\times(0.9,1) \cup (-1,-0.9)\times(-0.8,-0.7) \cup (-1,-0.9)\times(-0.1,0.1) \cup (-1,-0.9)\times(0.7,0.8)(0.9,1)\times(-0.8,-0.7) \cup (0.9,1)\times(-0.1,0.1) \cup (0.9,1)\times(0.7,0..8)$. We take $S_1 = \emptyset$. There shall be 51.25% material and 48.75% void. We display results from the same two sets of initial data as in the bridge simulation except we have $\boldsymbol{\varphi}_h^0 = (1,0)^T$ in S_0.

In Figures 10 and 12 we see that although the two sets of initial data give rise to different evolutions the final state solutions are the same. Since there can be many local minima, this is in fact not required. In Figures 11 and 13 we display the displacement vector $\mathbf{u}$ and in Figure 14 we display the deformed optimal configuration.

https://doi.org/10.1051/cocv/2014006 Published online by Cambridge University Press

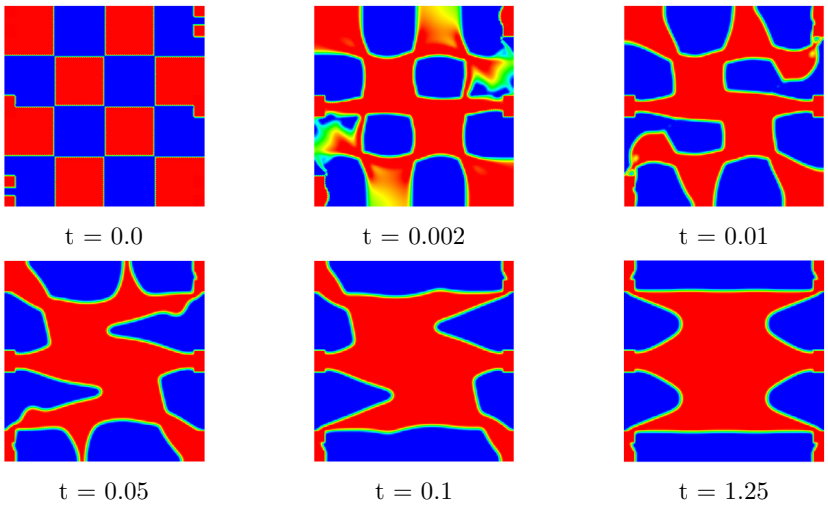


FIGURE 12. Push simulation with $N = 2$ and checkerboard initial data, material in red and void in blue.

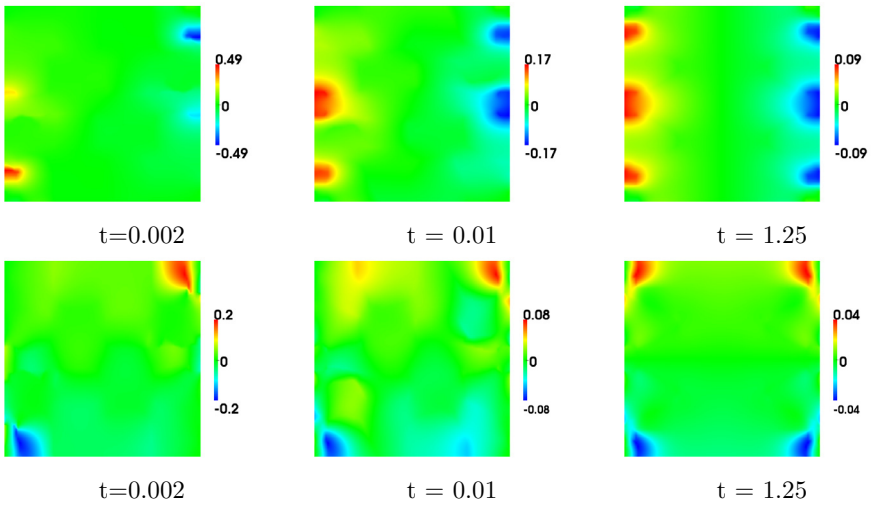


FIGURE 13. Displacement vector for the push simulation with $N = 2$ and checkerboard initial data; x-component top row, y component bottom row.

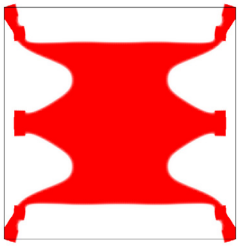


FIGURE 14. Deformed optimal configuration.

https://doi.org/10.1051/cocv/2014006 Published online by Cambridge University Press

7. Conclusions

A multi-material structural topology optimization problem has been formulated in a phase field context. First-order necessary optimality conditions are rigorously derived. They are formulated as a variational inequality since the material concentration functions are restricted to lie on the Gibbs simplex.

It is possible to relate the first-order conditions of the phase field approach to classical necessary conditions derived in the context of shape calculus by using formally matched asymptotic expansions. In particular, we can relate our results to the sensitivity analysis of [3]. In addition, at material-material interfaces we obtain terms generalizing the Eshelby traction from materials science, see (5.22).

Finally numerical simulations show that the approach can be used for mean compliance and for tracking type functionals. Topology changes and the creation of new holes are possible in the approach without using topological derivatives.

References

[1] H. Abels, H. Garcke and G. Grün, Thermodynamically consistent, frame indifferent diffuse interface models for incompressible two-phase flows with different densities. *Math. Models Methods Appl. Sci.* **22** (2012) 1150013.
[2] G. Allaire, *Optimization by the Homogenization Method*. Springer, Berlin (2002).
[3] G. Allaire, F. Jouve and A.-M. Toader, Structural optimization using sensitivity analysis and a level set method. *J. Comput. Phys.* **194** (2004) 363–393.
[4] S. Baldo, Minimal interface criterion for phase transitions in mixtures of Cahn−Hillard fluids. *Ann. Inst. Henri Poincaré* **7** (1990) 67–90.
[5] J.W. Barrett, H. Garcke and R. Nürnberg, On sharp interface limits of Allen−Cahn/Cahn−Hilliard variational inequalities. *Discrete Contin. Dyn. Syst. Ser.* **S1** (2008) 1–14.
[6] J.W. Barrett, R. Nürnberg and V. Styles, Finite Element approximation of a phase field model for void electromigration. *SIAM J. Numer. Anal.* **46** (2004) 738–772.
[7] M.P. Bendsoe and O. Sigmund, Topology Optimization. Springer, Berlin (2003).
[8] L. Blank, H. Garcke, L. Sarbu and V. Styles, Non-local Allen-Cahn systems: analysis and a primal dual active set method. *IMA J. Numer. Anal.* **33** (2013) 1126–1155.
[9] L. Blank, H. Garcke, L. Sarbu, T. Srisupattarawanit, V. Styles and A. Voigt, Phase-field approaches to structural topology optimization. *Constrained Optim. Opt. Control for Partial Differ. Eqs.*, edited by G. Leugering, S. Engell, A. Griewank, M. Hinze, R. Rannacher, V. Schulz, M. Ulbrich, S. Ulbrich. In vol. 160, *Int. Ser. Numer. Math.* (2012) 245–255.
[10] J.F. Blowey and C.M. Elliott, Curvature dependent phase boundary motion and parabolic double obstacle problems. *IMA J. Math. Appl.* **47** (1993) 19–60.
[11] B. Bourdin and A. Chambolle, Design-dependent loads in topology optimization. *ESAIM: COCV* **9** (2003) 19–48.
[12] B. Bourdin and A. Chambolle, The phase-field method in optimal design, in vol. 137 of *IUTAM Symposium on Topological Design Optimization of Structures, Machines and Materials* (2006) 207–215.
[13] L. Bronsard, H. Garcke and B. Stoth, A multi-phase Mullins-Sekerka system: matched asymptotic expansions and an implicit time discretization for the geometric evolution problem. *SIAM J. Appl. Math.* **60** (1999) 295–315.
[14] L. Bronsard, C. Gui and M. Schatzman, A three layered minimizer in $\mathbb{R}^2$ for a variational problem with a symmetric three-well potential. *Commun. Pure Appl. Math.* **47** (1996) 677–715.
[15] L. Bronsard and R. Reitich, On singular three-phase boundary motion and the singular limit of a vector-valued Ginzburg-Landau equation. *Arch. Rat. Mech. Anal.* **124** (1993) 355–379.
[16] M. Burger and R. Stainko, Phase-field relaxation of topology optimization with local stress constraints. *SIAM J. Control Optim.* **45** (2006) 1447–1466.
[17] M. Burger, A framework for the construction of level set methods for shape optimization and reconstruction. *Interfaces Free Bound.* **5** (2003) 301–332.
[18] M. Burger, B. Hackl and W. Ring, Incorporating topological derivatives into level set methods. *J. Comput. Phys.* **194** (2004) 344–362.
[19] J.W. Cahn and J.E. Hilliard, Free energy of a nonuniform system. I. Interfacial free energy. *J. Chem. Phys.* **28** (1958) 258–267.
[20] L.Q. Chen, Phase-field models for microstructure evolution. *Ann. Rev. Mater. Research* **32** (2002) 113–140.
[21] P.G. Ciarlet, Mathematical Elasticity, Three Dimensional Elasticity, vol. 1. Elsevier (1988).
[22] T.A. Davis, UMFPACK Version 5.2.0 User Guide. University of Florida (2007).
[23] K. Deckelnick, G. Dziuk and C.M. Elliott, Computation of geometric pdes and mean curvature flow. *Acta Numerica* (2005) 139–232.
[24] L. Dedè, M.J. Borden, T.J.R. Hughes, Isogeometric analysis for topology optimization with a phase field model, *Arch. Comput. Methods Eng.* **19** (2012) 427–465.
[25] C.M. Elliott and S. Luckhaus, A generalised diffusion equation for phase separation of a multi-component mixture with interfacial free energy. SFB256, Preprint 195, University Bonn (1999).

https://doi.org/10.1051/cocv/2014006 Published online by Cambridge University Press

[26] P.C. Fife, Dynamics of internal layers and diffusive interfaces. Vol. 53 of *CBMS-NSF Regional Conf. Ser. Appl. Math.* SIAM, Philadelphia (1988).
[27] P.C. Fife and O. Penrose, Interfacial dynamics for thermodynamically consistent phase-field models with nonconserved order parameter. *EJDE* (1995) 1–49.
[28] P. Fratzl, O. Penrose and J.L. Lebowitz, Modeling of phase separation in alloys with coherent elastic misfit. *J. Statist. Phys.* **95** (1999).
[29] H. Garcke, The Γ-limit of the Ginzburg-Landau energy in an elastic medium. *AMSA* **18** (2008) 345–379.
[30] H. Garcke, On Cahn−Hilliard systems with elasticity. *Proc. Roy. Soc. Edinburgh Sect. A* **133** (2003) 307–331.
[31] H. Garcke, B. Nestler and B. Stoth, On anisotropic order parameter models for multi-phase systems and their sharp interface limits. *Phys. D* **115** (1998) 87–108.
[32] H. Garcke, B. Nestler and B. Stoth, A multi phase field concept: numerical simulations for moving phase boundaries and multiple junctions. *SIAM J. Appl. Math.* **60** (1999) 295–315.
[33] H. Garcke and A. Novick-Cohen, A singular limit for a system of degenerate Cahn−Hilliard equations. *Adv. Differ. Eqs.* **5** (2000) 401–434.
[34] H. Garcke, R. Nürnberg, V. Styles, Stress and diffusion induced interface motion: Modelling and numerical simulations. *Eur. J. Appl. Math.* **18** (2007) 631–657.
[35] H. Garcke and B. Stinner, Second order phase field asymptotics for multicomponent systems. *Interfaces Free Boundaries* **8** (2006) 131–157.
[36] M. Giaquinta and L. Martinazzi, An introduction to the regularity theory for elliptic systems, harmonic maps and minimal graphs. Edizioni della normale, Scuola Normale Superiore Pisa (2005).
[37] M.E. Gurtin. An introduction to continuum mechanics. *Math. Sci. Engrg.* **158** (2003).
[38] I. Hlavacek and J. Necas, On inequalities of Korn's type, I. Boundary value problems for elliptic systems of partial differential equations. *Arch. Rat. Mech. Anal.* **36** (1970) 312–334.
[39] F.C. Larché and J.W. Cahn, The effect of self-stress on diffusion in solids. *Acta Metall.* **30** (1982) 1835–1845.
[40] L. Modica, The gradient theory of phase transitions and minimal interface criterion. *Arch. Rat. Mech. Anal.* **98** (1987) 123–142.
[41] F. Murat and S. Simon, Etudes des problèmes d'optimal design. *Lect. Notes Comput. Sci.* Springer Verlag, Berlin **41** (1976) 54–62.
[42] A. Novick-Cohen and L. Peres Hari, Geometric motion for a degenerate Allen−Cahn/Cahn−Hillard system: The partial wetting case. *Physica D* **209** (2005) 205–235.
[43] O.A. Oleinik, A.S. Shamaev and G.A. Yosifian, Mathematical problems in elasticity and homogenization. In vol. 26 of *Studies Math. Appl.* (1992) 1–398.
[44] S.J. Osher and F. Santosa, Level set methods for optimization problems involving geometry and constraints. I. Frequencies of a two-density inhomogeneous drum. *J. Comput. Phys.* **171** (2011) 272–288.
[45] S.J. Osher and J.A. Sethian, Fronts propagating with curvature-dependent speed: algorithms based on Hamilton-Jacobi formulations. *J. Comput. Phys.* **79** (1988) 12–49.
[46] N. Owen, J. Rubinstein and P. Sternberg, Minimizers and gradient flows for singularly perturbed bi-stable potentials with a Dirichlet condition. *Roc. Roy. Soc. London A* **429** (1990) 505–532.
[47] J. Petersson, Some convergence results in perimeter-controlled topology optimization. *Comput. Meth. Appl. Mech. Eng.* **171** (1999) 123–140.
[48] O. Pironneau, Optimal Shape Design for Elliptic Systems. Springer-Verlag, New York (1984).
[49] J. Rubinstein and P. Sternberg, Nonlocal reaction-diffusion equations and nucleation. *IMA J. Appl. Math.* **48** (1992) 249–264.
[50] P. Penzler, M. Rumpf and B. Wirth, A phase-field model for compliance shape optimization in nonlinear elasticity. *ESAIM: COCV* **18** (2012) 229–258.
[51] A. Schmidt and K.G. Siebert, Design and adaptive finite element software. The finite element toolbox ALBERTA. In vol. 42 of *Lect. Notes Comput. Sci. Eng.* Springer-Verlag, Berlin (2005).
[52] O. Sigmund, J. Petersson, Numerical instabilities in topology optimization: A survey on procedures dealing with checkerboards, mesh-dependencies and local minima. *Struct. Multidisc Optim.* **16** (1998) 68–75.
[53] J. Simon, Differentiation with respect to domain boundary value problems. *Numer. Funct. Anal. Optim.* **2** (1980) 649–687.
[54] J. Sokolowski and J.P. Zolesio, Introduction to shape optimization: shape sensitivity analysis, vol. 10. *Springer Ser. Comput. Math.* Springer, Berlin (1992).
[55] A. Takezawa, S. Nishiwaki and M. Kitamura, Shape and topology optimization based on the phase field method and sensitivity analysis. *J. Comput. Phys.* **229** (2010) 2697–2718.
[56] F. Tröltzsch, Optimal control of partial differential equations: theory, methods and applications, vol. 112. *Graduate Studies Math.* (2010).
[57] J.D. van der Waals, The thermodynamic theory of capillarity under the hypothesis of a continuous variation of density (in Dutch), Vol. 1. Verhaendel. Kronik. Akad. Weten. Amsterdam (1983); Engl. translation by J.S. Rowlinson. *J. Stat. Phys.* **20** (1979) 197–244.
[58] M. Wallin and M. Ristinmaa, Howard's algorithm in a phase-field topology optimization approach. *Int. J. Numer. Meth. Eng.* **94** (2013) 43–59.
[59] M.Y. Wang and S.W. Zhou, Phase field: A variational method for structural topology optimization. *Comput. Model. Eng. Sci.* **6** (2004) 547–566.

https://doi.org/10.1051/cocv/2014006 Published online by Cambridge University Press

[60] M.Y. Wang and S.W. Zhou, Multimaterial structural topology optimization with a generalized Cahn−Hilliard model of multiphase transition. *Struct. Multidisc. Optim.* **33** (2007) 89-111.
[61] M.Y. Wang and S.W. Zhou, 3D multi-material structural topology optimization with the generalized Cahn−Hilliard equations. *Comput. Model. Eng. Sci.* **16** (2006) 83–102.
[62] E. Zeidler, Nonlinear Functional Analysis and its Applications, I: Fixed-point theorems. Springer-Verlag (1986).
[63] E. Zeidler, Nonlinear Functional Analysis and its Applications, IV. Applications Math. Phys. Springer Verlag (1988).
[64] E. Zeidler, Nonlinear Functional Analysis and its Applications, II/B. Nonlinear Monotone Operators. Springer Verlag (1990).
[65] J. Zowe and S. Kurcyusz, Regularity and stability for the mathematical programming problem in Banach spaces. *Appl. Math. Optim.* **5** (1979) 49–62.

https://doi.org/10.1051/cocv/2014006 Published online by Cambridge University Press